Enhancing the Water Solubility of MyoNovin - a novel skeletal muscle regenerator

by

Siyan Wang

A Thesis Submitted to the Faculty of Graduate Studies of

The University of Manitoba

in partial fulfillment of the requirements of the degree of

MASTER OF SCIENCE

Faculty of Pharmacy

University of Manitoba

Winnipeg

Acknowledgment

My deepest gratitude goes first and foremost to Dr. Frank Burczynski, my supervisor, for his patients and invaluable supervision provided during the course of this work. He has walked me through all the stages of the writing of this thesis. Without his consistent and illuminating instruction, this thesis could not have reached its present form.

Second, I would like to express my heartfelt gratitude to Dr. Geoffrey Tranmer, Dr. Judy Anderson, Dr. Neal Davies and Dr. Dennis Cote for their concern, support, and many interesting discussions during the course of this work. Their encouragement, understanding and advice have led me through many hard decisions and difficult times.

Special thanks also go to Haoyue Zhang from Dr. Anderson's lab, Drielly Braite and Sarah Eloi who were summer students with Drs Burczynski and Anderson, and all my colleagues in the Faculty of Pharmacy for their help and support.

Last but not least, I want to thank my parents and families, Chao Wang, Anqing Lu and Bing Hu, who have always been extremely caring and supportive to me.

ABSTRACT

Satellite precursor cells are normally quiescent but once activated they support skeletal muscle growth and regeneration by proliferating and differentiating into myoblasts. When an animal suffers from a muscle injury, quiescent satellite precursor cells are activated by nitric oxide (NO). MyoNovin (1-(3,4-Bis-nitrooxy-butoxy)-2-methoxy-benzene), as a NO donor, was developed to provide nitric oxide directly to the skeletal muscle and has been shown to promote satellite cell activation. A potential drawback of the current MyoNovin molecule is its poor water solubility. The aim of this work was to enhance the water-solubility of MyoNovin in order to improve its ease of formulation and possibly enhance its biological activity. The structure of MyoNovin (MN1) was modified with three different functional groups - methanesulfonyl (MN2), benzoic acid (MN3) and acetamide (MN4). The three novel MyoNovin analogs were identified and shown to have similar biological activity as with MyoNovin. All three MyoNovin analogs were found to have better water solubility. Based on these results, two of the MyoNovin analogs (MN2 and MN3) had much better biological activity with respect to satellite activation and much improved water solubility and may be the most promising candidates for future studies.

Table of Contents

List of Figures

List of Tables

I. Introduction

A: Introduction of Muscle injury

Muscle injury occurs when a muscle or tendon is twisted, pulled and/or torn during an activity or movement. There are many different causes for muscle injury including overusing a muscle, performing intense exercises, or being infected with certain types of bacteria, viruses or parasites. Following injury, use of the injured muscle is often limited and this lack of use may lead to loss of muscle mass and subsequent atrophy. Atrophy is associated with a decline in overall muscle function and poor muscle function can lead to loss of mobility. The affected person is more likely to be injured when suffering from a fall or even from daily activities such as lifting heavy objects or just going up and down stairs. Twenty six percent of Canadians aged 65 and over self-reported a fall resulting in injury while going up or down stairs [1]. As elderly people have lower recuperative abilities compared with younger individuals，they need to receive more attention for muscle injury and other fall-related conditions such as hip fractures [1]. The rate of fall-related injuries in the elderly is nine times more than those under 65 years of age [1]. Injury from falls therefore has a dramatic impact on their quality of life.

Muscle weakness and the resulting falls are one of the biggest health risks as people age. In 2009, adults aged 65 years and older accounted for 14% of our population [2]. It is estimated that

approximately 28-35% of people in this age range may fall at least once a year. There is an 10% increase in the rate of falls for each decade over 70 years of age [3,4]. In the report "Seniors' falls in Canada", the authors claim almost half of the seniors age 65 and over fall at least once annually [1]. The far-reaching impact of falls among seniors has been recognized at personal, family and societal levels. For those older people who have sustained a fall, the long-term effects of these injuries may impact their independence and self-confidence leading to a reduced quality of life. As they usually are incapacitated, the elderly are more likely to depend on their families for support. Fall related injuries could also have significant economic healthcare consequences because of the cost associated from hospitalization or nursing home long-term care. These healthcare costs are approximately $2.0 billion annually and growing year by year [5].

Among older individuals, fall-related injuries are the major causes of sprains, strains, fractures, hospital admissions from trauma, and even death. Sprains, fractures and scrapes are the most common fall-related injuries in seniors, which account for 36.6%, 25.9% and 11.9%, respectively [3]. Among these injuries, seniors are much more likely to suffer from fractures than those under the age of 65 and women are at more risk, accounting for 75–80% of all hip fractures. A hip fracture can result in serious disability and contributes to both morbidity and mortality in the elderly. In 2008, 15.5 per 1,000 elderly Canadians aged 65 and over were hospitalized for a fall-related injury [6]. This number is approximately two times higher than the average of all

Canadians, making falls the number one cause of injury-related hospital admission for the elderly [1]. The analyses provided by Canadian Vital Statistics shows that for the six years ending in 2002, the number of direct deaths resulting from a fall was approximately 7500 for Canadians age 65 and over. This number increased by 30% from 1997-1999 to 2000-2002. This number also increases with age and more than half are seniors aged 85 and over.

Falls result from a complex interaction of risk factors. Although vision changes and chronic illness can contribute to falling, lose of muscle mass and strength is still the basic and most important factor. Loss of muscle mass and strength naturally occurs during the aging process but besides age, other factors affecting muscle include diseases and inactivity. Scientists have classified muscle mass loss into three categories - sarcopenia, cachexia, and atrophy – by different causes that are explained below.

Sarcopenia was first defined by Irwin Rosenberg in 1988, as the progressive loss of skeletal muscle mass associated with aging [5]. Sarcopenia is considered to be responsible for limiting physical activity by an individual through losing muscle strength resulting in increased falls and potentially hip fractures in seniors. Sixty percent of the body's protein is stored in various forms, such as actin, myosin, regulation proteins and contractile proteins in the skeletal muscle. As neuromuscular function and performance decrease significantly during the aging process, skeletal muscle mass and muscle strength decrease inevitably even in healthy aging [7]. The most

common predisposing factors for sarcopenia are decreased level of physical activity, malnutrition and most importantly cachexia, which links muscle loss to disease [8]. The major clinical manifestation of sarcopenia is low muscle mass, low muscle strength and low physical performance. Sarcopenia also affects organ function, leading to heart and lung failure and even death [9].

Cachexia links various chronic diseases such as cancer, AIDS and other acute medical conditions with tremendous body weight loss and muscle weakness [8]. This condition cannot be reversed even if extra calories are provided. Lean mass will continue to decline due to the underlying disorder. Actomyosin, actin, and myosin are considered to be the degradation targets in cachexia [10-12]. Based on Acharyya's study, the heavy chain of myosin is the selective target for cachectic factors. In their investigation, two markers of inflammation, TNF-α and IFN-γ, are found to be the strongest cachectic factors in reducing myosin expression. Studies have shown that TNF-α and IFN-γ are increased in mice with colon-26 tumors and associated with this increase was a decrease in the expression of myosin [10]. Other potential mediators are affected and are dependent on the underlying disease. These mediators include testosterone [13], insulin-like growth factor I (IGF-I) [14], myostatin [15], adrenal hormones [16], and leptin [17]. For example, serum levels of testosterone will decrease in patients with type 2 diabetes [15].

Muscle atrophy normally occurs when there is a lack of physical activity. Muscle atrophy is

common during fractures and is due to physical immobility while the bone heals. Sometimes, sarcopenia, cachexia and atrophy can occur simultaneously and the ultimate therapeutic goal in these conditions is to maintain muscle mass. The treatment for sarcopenia is mainly focused on exercise. As exercise intervention is likely to prevent and even reverse the muscle atrophy that comes with aging [18]. There are no effective and safe pharmaceuticals or supplements to treat sarcopenia so drugs that can promote muscle regeneration may become an important and active research area. With having access to such medications, healthier aging and elderly having a better quality of life would become evident.

B: Skeletal Muscle Regeneration

Skeletal muscle has a robust capacity for maintaining working skeletal musculature function through the process of regeneration. Muscle regeneration is seen as an adaptive response to injury or disease, such as cancer, heart failure and other chronic diseases [19], that forms new myofibers and reconstitutes functional contractility. However, during the aging process, muscle mass decreases due to atrophy and the ability to replace the lost muscle mass also diminishes. A solid understanding of the cellular and molecular mechanisms of muscle regeneration aids in the development of novel muscle regenerating drugs. The first research on the response of skeletal

muscle to injury, which did not believe that muscle regeneration existed, was published in the mid-19th century [20]. Following this initial publication more than one hundred years of investigation into muscle physiology/biochemistry has led to a good understanding of the regenerative process. The discovery of satellite cells adjacent to the myofiber is considered as the landmark event in the development of muscle regeneration theory by Mauro [21]. A wealth of studies on satellite cells has clarified the cellular and molecular mechanisms in the muscle regenerative process. Those studies also gave direction to the treatment strategy that may reduce the symptoms related to poor muscle regenerative ability, especially in the normal aging process. Several lines of evidence working on satellite cells explain the basic mechanism and characterize different factors contributing in the regeneration process[21-23]. Section 1 describes the major features of adult skeletal muscle while Section 2 gives a detailed description of skeletal muscle regeneration and activation of satellite cells. The studies in Section 3, on nitric oxide in skeletal muscle regeneration, have led to a particular interest in possessing potent growth-promoting or growth-inhibiting activities on skeletal muscle.

1. Muscle Physiology

Muscles, which are highly efficient at converting chemical energy directly into mechanical

energy, evolved to allow precise movements in animals. These movements are the result of unique characteristics of skeletal muscle cells. The contractile cells of the body can be classified into three major groups: skeletal, cardiac and smooth muscle cells. These three types of cells can be distinguished on the basis of their shape, number of nuclei, position of nuclei, presence of striations, and whether they are under voluntary or involuntary control. There are approximately 640 skeletal muscles in the human body, which collectively account for 38% and 30% of total body mass for men and women, respectively [24]. Skeletal muscle, which is under voluntary control, has an elongated cell with multiple peripheral nuclei. While cardiac muscle cells have branched cells with a single central nucleus. Unlike skeletal muscle, cardiac muscle cells are under involuntary control. Smooth muscle cells possess a single central nucleus within a spindle-shaped cell. These cells do not have visible striations and like cardiac muscle, smooth muscle is under involuntary control. Studies indicate that skeletal muscle fascicle is the basic contractile unit of skeletal muscles, orderly surrounded by connective tissue layers and combined to become bundles forming skeletal muscles (see Figure 1). The entire muscle is surrounded by an external connective tissue wrapping, which is called the epimysium. Within the fascicle, the third connective tissue layer, the endomysium, separates and electrically insulates muscle cells from each other. All three connective tissue layers - endomysium, primysium and epimysium – bind the muscle cells together, providing strength and support to the entire muscle. A myofibril

is a cylindrical bundle of contractile filaments within the skeletal muscle cell. The myofibrils that are packed into a muscle cell are composed of individual contractile proteins called myofilaments. There are two types of myofilaments: the thin filament is composed mainly of the protein actin, and the thick filament is made up chiefly of the protein myosin. The arrangement of thick and thin myofilaments, a bundle-within-a-bundle organization from myofilaments to myofibrils to muscle fibers to fascicles constitutes the whole muscle. In order to provide essential nutrients for muscle function, skeletal muscles are rich in blood vessels. The functional properties of skeletal muscle are therefore due to the complex combined effect of myofibers, motor neurons, blood vessels, and extracellular connective tissue matrix.

Each muscle fiber is formed during embryonic development and continues to grow throughout an animal's life and all vertebrate skeletal muscles cells, excluding those of the head, are derived from the paraxial mesoderm. Paraxial mesoderms differentiate into somites that are arranged in pairs on both sides of the embryonic neural tube. In mice, somite development starts at the eighth day of embryonic development. Somites can differentiate into chondrocytes, fibroblasts, angioblast and skeletal muscle precursor cells-myoblasts [25].

Figure 1. Muscle Structure.

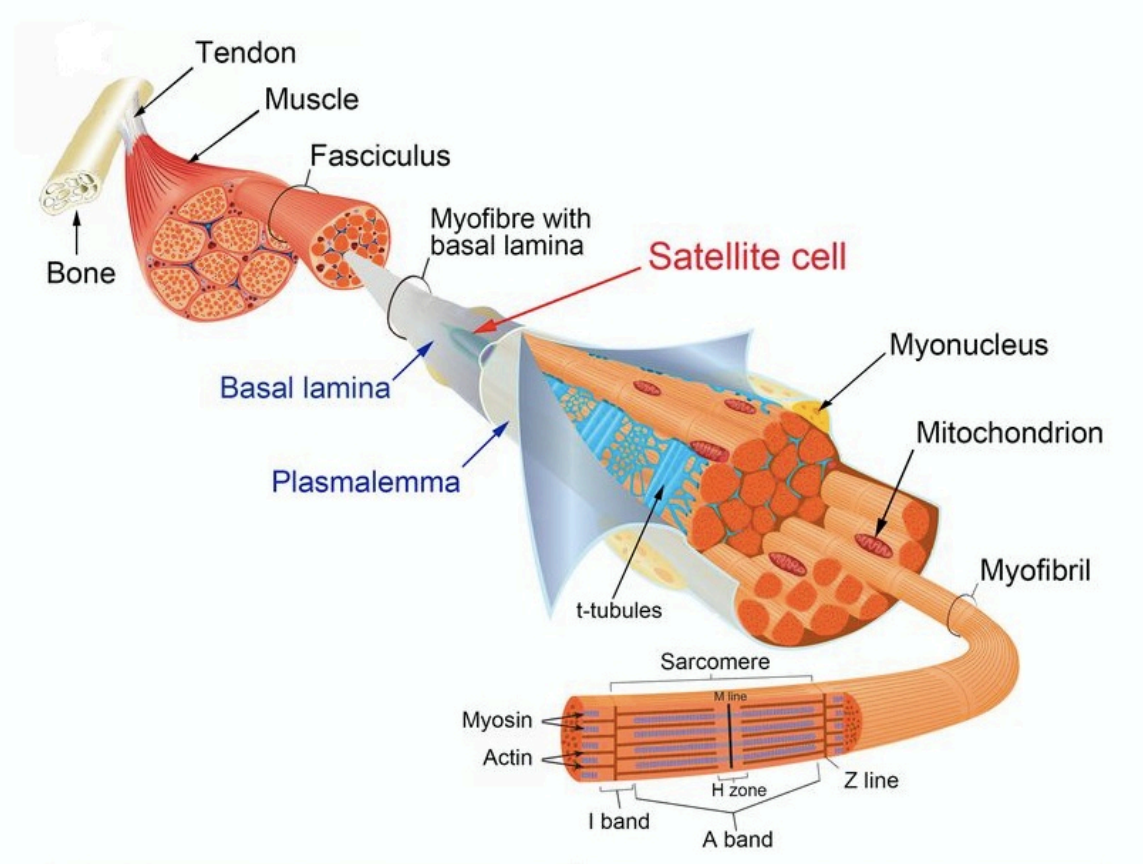

The structure and ultra-structure of skeletal muscle [23]. The satellite cell is shown on the surface of the myofibre, beneath the surrounding basal lamina. Figure has been modified from S. Tajbakhsh, 2004 on October 2009 with the permission from © John Wiley and Sons.

When somites further develop, the ventral part of the somites start epithelial-mesenchymal transformation to form the sclerotomes which will develop into the cartilage, vertebra and ribs; the dorsal part of the somite remains epithelial tissue, forming dermomyotome. The dorsal part of the dermomyotome will develop the trunk dermis; the central part will continue to develop downward and form the myotome, which differentiates quickly into muscle cells and merges into myotubes. The central part of dermomyotome forms the epaxial muscle while the lateral part will develop into both hypaxial muscles and the skeletal muscle of limbs [26]. Somite myotome area produces muscle precursor cells that are also called myoblasts. Myoblasts，mononuclear fusiform cells, are capable of DNA replicating and cell division. When reaching a certain stage, proliferating myoblasts withdraw from the cell cycle to become terminally differentiated myocytes. Myocytes lose the ability of DNA replication and cell division and fuse together to form multi-nucleated fiber. After embryonic development, some myoblasts return to quiescence and become satellite cells.

2. Skeletal Muscle Regeneration

The skeletal muscle regenerative process may be initiated in response to a muscle injury. Skeletal muscle injury and the regeneration response is a highly coordinated process which can

be divided into different stages [27]. These stages include skeletal muscle degeneration with structural destruction of muscle fibers, infiltration of inflammatory cells, and finally satellite cell activation and proliferation to form new myotubes, which then develop into muscle fibers. Muscle regeneration depends on the balance between pro-inflammatory and anti-inflammatory factors, which determines whether damaged tissue can be fully recovered or if damage results in an accumulation of scar tissue. Based on current research, even for less severe injuries, the muscle self-repair ability is not totally efficient. Uncompleted natural repair processes will happen when more than twenty percent of muscle tissue is lost or muscle damaged by trauma. Under these conditions, scar formation will affect the reconstitute of the functional contractile apparatus [28].

2.1 Skeletal Muscle Degeneration

Studies show that the majority of injuries affecting skeletal muscle proceed in a similar manner regardless of the debilitating condition the patient suffers [22,29]. After muscle injury, due to sarcolemmal or sarcoplasmic reticulum damage, the damaged area loses calcium homeostasis. The calcium influx in this area is increased and calcium-dependent proteolysis is increased correspondingly [30]. This initiates the protein degradation system in muscles. Activation of the Ca^{2+}-dependent calpain protein degradation system is one of the major ways to degrade

intracellular protein. Calpains can cleave myofibrils and cytoskeletal proteins and also cause accelerated absorption of internal damage tissue in the muscle fiber. This process can contribute to the regeneration response in the injured site. Moreover, with an increasing concentration of free Ca^{2+} in the cytosol, phospholipase A2 is activated [31]. These changes disrupt the normal function of mitochondrial and other membrane phospholipids and increase the amount of lysopholipids and free fatty acids. Lysophospholipids are capable of disrupting membrane lipid organization and the elevated free fatty acids will cause membrane damage. As a result, myofibrils rupture, mitochondria break and sarcolemma damage occurs.

In the early stages of muscle damage, muscle regeneration is always accompanied by infiltration of the damaged muscle by inflammatory cells. The activation of mono-nucleated cells, principally inflammatory cells and myogenic cells, are present one to six hours after muscle damage and remain for the next few days [32]. This complex response ceases after the injury is cleared of all impaired tissue.

Approximately 48 hours after the injury, the dominant inflammatory cells in injured muscle are macrophages. These cells migrate through the bloodstream to the damaged area. After infiltration, macrophages phagocytize cell debris and destroy myofibrils, other cytoplasmic structures and damaged sarcolemma. Furthermore, macrophages activate myoblasts. The ability of phagocytic function will directly affect whether the damage tissue can be repaired completely

or not at all [33]. Moreover, a small amount of neutrophils and other blood-derived cells have infiltration features as well that spread to the injury site, phagocytizing damage muscle tissue and dead cells. It should be noted that the infiltration function of these blood-derived cells could only work after revascularization is complete at the site of injury [22]. As the injury site itself may cause blood circulation disorders that may block blood supply to the injured tissue, the delays and prevention of the infiltration always occur, which relate to the delay in repair. It is undeniable that in the early stages of muscle damage, the main histopathological features are muscle fiber necrosis and an increase in the number of monocytes in non-muscle injured area.

2.2 Satellite Cell in Muscle Regeneration

2.2.1 Satellite Cell

Mammalian skeletal muscles strongly adapt to stimuli such as growth, exercise, and injury. This process occurs mainly due to the presence of satellite cells. In 1961, Mauro described cells closely attached to the edge of frog muscle fiber cells and named them satellite cells according to their location, which is between the sarcolemma and basement membrane. The Annual Meeting of American College of Sports Medicine [34] had highlighted that satellite cells and growth factors have important roles in skeletal muscle growth, development, adapted training, injury and transplantation. Satellite cells are small spindle-shaped cells with a prominent nucleus and a low

volume of organelles. Under normal circumstances, about 2% of myofiber nuclei are satellite cells and these cells do not divide and remain stationary. There are two main factors, myostatin [35] and caveolin-1 [36], that inhibit satellite cell proliferation in order to achieve cellular senescence. Myostatin is a member of the transforming growth factor beta (TGF-β) family. Evidence shows that the number of proliferating satellite cells is increased in myostatin knock-out mice. The research indicated that apart from the activated satellite cells, acceleration of phagocytotic cells and invasion and removal of inflammation might also be a reason for the enhancement of muscle regeneration. Another factor caveolin-1 is expressed in satellite cells but not in muscle fibers. Caveolin-1 function is regulated by hepatocyte growth factor (HGF). HGF is considered to be produced following muscle injury and is one of the principal initiators of satellite cell proliferation. In adult muscle stimulated by muscle injury or exercise, satellite cells will be activated, proliferate and differentiate to form muscle cells. Eventually， these cells fuse with the original skeletal muscle cells or add to the rear of the muscle fibers after fusing into myotubes and form the new muscle fibers [22,37]. Although satellite cells exist in all skeletal muscles, the size of their population is different in each muscle and also in relation to age and mitotic activity [38]. Within the same muscle, satellite cells are more likely to be found near slow muscle fibers rather than fast muscle fibers. Analogously, Kelly reported in some muscle tissue, such as the soleus, that most satellite cells occur adjacent to the neuromuscular junctions on fibers [39].

2.2.2 Satellite Cell activation

Muscle injury causes muscle fiber necrosis, which leads to satellite cell proliferation in dying tissues. Satellite cells are activated while the damaged muscle tissue degenerates and the inflammation reaction is occurring. Evidence for this is based on observations at 5, 10 and 30 minutes after injury [37]. Nitric oxide starts to be released and satellite cells are observed to emerge and their nuclei become enlarged. DNA synthesis increases, cytoplasmic content increases and cytoplasmic density rises, which indicate that satellite cells have been activated and they begin to exhibit division and proliferation properties. Cornelison concluded that the proliferation of satellite cells in damaged muscle starts after one day [40] and Bischoff pointed out that it could occur as early as 18 hours following injury [41].

When studying the tropism of satellite cells, Bischoff [41] reported that migration of the myogenic cells is very extensive. It is noteworthy that just a few satellite cells migrate to the injury site from undamaged tissues [42]. Damage causes adjacent satellite cells to proliferate but the muscles near the damaged site also degenerates [42]. When the conjunctive tissue of muscle membrane structure is damaged, satellite cells in adjacent muscle fibers will migrate to the site of injury [42].

Under normal circumstances, satellite cells remain dormant and that is the reason why they are also known as dormant myoblasts [41]. Satellite cell activation generally appears after

macrophages begin to phagocytosis necrotic fibers, which suggests satellite cell activation depends on certain substances secreted by macrophages. indicating that there are other factors regulating satellite cell activation [43]. Several factors are found to be important in regulating the activation process of satellite cell. The intracellular signal may be provided by sphingosine (S1P) within the cell membrane. S1P，the intermediate product for membrane phospholipid metabolism, is an important factor for satellite cells entering the cell cycle and skeletal muscle regeneration [44]. S1P serves as a muscle trophic factor and was reported to enhance satellite cell activation through a S1PR2/STAT3 signaling pathway [45]. When its synthesis is restricted, the number of satellite cells entering the cell cycle is reduced.

Figure 2. Electronmicrographs of satellite cells

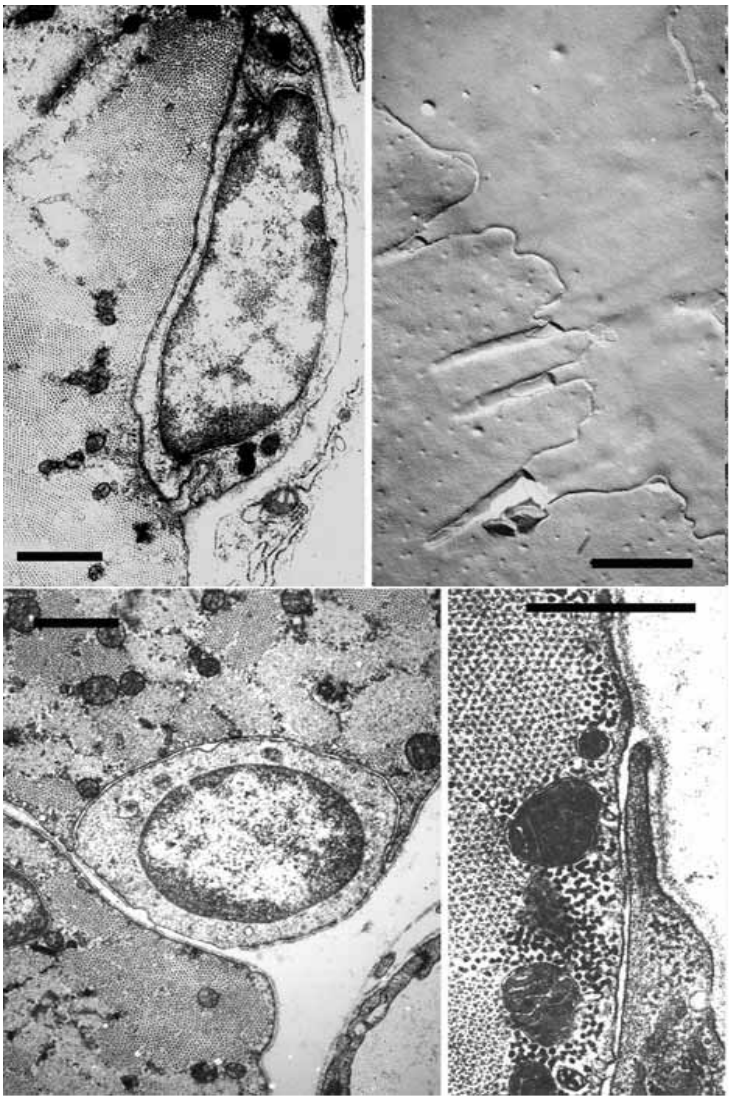

Top left: Quiescent satellite cells of normal rat soleus muscles. Top right: Freeze-Fracture of a satellite cell from a rat soleus muscle. Lower left: Activated satellite cell of a regenerating rat soleus muscle. Lower right: Human brachial biceps muscle. Figure adopted from Mauro, A, 1961 on June 5, 2014 with the permission from ©1961. Rockefeller University Press. Journal of Biophysical and Biochemical Cytology. 9:493-495.

Mechanical stretching of muscle fibers also causes intracellular signal transduction, including the synthesis of NO, which can lead to hepatocyte growth factor (HGF) release and activation of satellite cells. This means that the HGF receptor c-Met may be the gene triggering the early activation of satellite cells [46]. NO also promotes the expression of Folistatin [47], which may result in satellite cells to exit the resting state. Growth factors in the cellular microenvironment are the third class of factors that can activate satellite cells. In fact, fibroblast growth factors can trigger p38 mitogen-activated protein kinase (MAPK) signal transduction and phosphatidylinositol 3-kinase (P13K). This signal can activate satellite cells and regulate the resting state of satellite cells [48]. From the perspective of molecular biology, activation, cleavage and proliferation of satellite cells and the final formation into mature muscle fibers is a very complex process that includes：the regulation of skeletal muscle regeneration by a variety of biological factors such as insulin-like growth factor (IGF), hepatocyte growth factor (HGF), fibroblast growth factor (FGF), and leukemia inhibitory factor (LIF) [42,49-54]; the regulation function of specific muscle differentiation control gene MYOD family in skeletal muscle regeneration [49,52]; changes of myosin heavy chain (MHC) isoforms in muscle regeneration process and its effect to differentiating muscle fibers; the role of microfilaments and extracellular matrix in skeletal muscle regeneration [51]; and the relationship between skeletal muscle regeneration and degeneration. A study published by Daniel C. Bowers et al. [54] also found that in

the process of muscle fiber regeneration, not only satellite cells in necrotic sites are involved in the repair response, satellite cells of the entire muscle can migrate into necrotic areas to be involved in the repair response. Moreover, the muscle satellite cells in normal muscle fibers that surround necrotic fibers may migrate to the necrotic areas and thus are involved in muscle regeneration [50,51]. Throughout the process of skeletal muscle regeneration, macrophage phagocytosis of necrotic tissue and satellite cell activation are the two most important stages that determine regeneration.

3. Role of NO in Muscle Regeneration

Nitric oxide, a signal transduction molecule with low molecular weight, is synthesized from L-arginine and oxygen by nitric oxide synthase (NOS) in vivo. Nitric oxide synthase has three isofoms in muscle: Neuronal NOS (nNOS), Inducible NOS (i-NOS) and Type III Endothelial NOS (e-NOS). The processes of nNOS (neuronal NOS) or eNOS (endothelial NOS) mediating nitric oxide production are controlled by the calcium-calmodulin. Unlike those, the inducible isoform, iNOS, produces NO by an immune defense mechanism and is only effective after being activated when cells are stimulated.

Expression levels of iNOS in skeletal muscle injury are related to the degree of

inflammation. Expression of iNOS was significantly increased in acute skeletal muscle injury, chronic persistent disorders, autoimmune inflammatory myopathy or other stress conditions, but not in normal muscles [55]. Moreover, after human and animal muscle cells exposed to lipopolysaccharide or inflammatory chemokines such as IL-1α, IFN-α, INF-β, IFN-γ and TNF-α, expression of iNOS is significantly increased [56]. The expression of iNOS has been found to have its own function only when tissues were inflamed. Many studies have shown that inhibition of all NOS isoforms impede muscle regeneration [57,58]. Rubinstein [59] and his group believe that when skeletal muscle injury results from crush injuries and ischemia-reperfusion injury, the expression delay of iNOS can increase the degree of damage in muscles and even cause rhabdomyolysis. They observed that in animal models of crush injury, iNOS expression was significantly increased in impaired skeletal muscle within 72 hours. They also reported that the expression of eNOS increased significantly. It may due to the vasodilation function of NO increasing the microcirculation of damaged areas. A study published by Elena Rigamonti [60] related iNOS expression with macrophages in the injured muscle and demonstrated that iNOS expression controls the homeostatic response. iNOS realizes this function by regulating satellite cell function and shaping the inflammatory infiltrate, which means that iNOS-expressing macrophages play an irreplaceable role in inflammation-dependent muscle healing.

Endothelial NOS (eNOS) is a nitric oxide synthase that produces NO in blood vessels.

eNOS, as a peripheral membrane protein, has been found in human muscles. The eNOS plays an important role in regulating vascular tone by inhibiting smooth muscle contraction and platelet aggregation. As eNOS is not related to muscle regeneration, further details are not discussed.

NO plays several important roles in skeletal muscle, including controlling muscle contractility and local blood flow [61]. Additionally, high levels of nNOS are present in the skeletal muscle, where NO regulates the synaptic signaling and plasticity [62]. In skeletal muscle physiology, NO exerts its effects by activating a series of downstream signaling cascades, which culminate in triggering skeletal muscle responses to injury. These downstream signaling cascades include: (1) activation of NO-dependent guanylyl cyclase in order to form cyclic GMP (cGMP); (2) redistribute oxygen by inhibiting cytochrome c oxidase in the mitochondrial respiratory chain; (3) S-nitrosylation (SNO) that covalently bind to a nitrogen monoxide group of cysteine's in class I histone deacetylase HDAC2 at positions 262 and 274 [63].

cGMP regulates NO-dependent vasodilation and vascular responses and maintains muscle homeostasis by controlling the complex intracellular signaling pathway through controlling calcium homeostasis [64]. Nitric oxide is believed to be the active substance that is responsible for generating cGMP, while cGMP shows the ability to reduce [Ca^{2+}]. By doing this, the enzyme that participates in smooth muscle cell contraction such as myosin light chain is inhibited [65]. Moreover, cGMP also activates the pathway that involved with sirtuin 1, the nuclear respiratory

factor 1 and the mitochondrial transcription factor A [66]. These processes play key roles in mediating NO-dependent biogenesis of mitochondria, which is accompanied by increased expression of the nuclear respiratory factor 1 and mitochondrial transcription factor A and ultimately leads to enhancement of ATP generation by skeletal muscles [67]. The main result of this process is to adjust the metabolism of the skeletal muscle cell to adapt to the low oxygen surroundings where satellite cell proliferation is being enhanced [68]. This process only happens with low concentrations of NO and can be fully reversed when NO is removed.

S-nitrosylation regulates the activity of several enzymes that function in skeletal muscles such as oxidoreductases, phosphatases and caspases [69]. In addition, several transcription factors, such as p53 and NF-κB are controlled by S-nitrosylation [70]. The most important function of S-nitrosylation in skeletal muscle is regulating the oxygen supply to mitochondria by controlling the interaction between oxygen and haemoglobin [56].

The mechanism of NO's function in skeletal muscle can be divided into two categories: (1) when the local concentration of NO is less than 1μmol/L; NO can react or combine with many molecules directly to exert its physiological or protective role [71]; (2) in inflammatory injury and other pathological conditions, lipopolysaccharides (LPS), interferon gamma (IFN-γ), interferon alpha (INF-α), interferon beta (INF-β) and interleukin-1 alpha (IL-1α) or other inflammatory chemokines may work together to induce expression of iNOS in skeletal muscle, which can

cause a sudden rise in NO concentration in the local area. Extra NO can react with oxygen free radicals to produce reactive nitrogen oxide species (RNOS), which are important in pathological damage and regeneration of skeletal muscles. Studies show the link between age-related muscle loss and increased ROS production [72]. Moreover, induction of myoblasts from glutathione peroxidase 1 knockout (Gpx1-/-) mice to differentiate into fused multinucleated myotubes, the result showed that the myotubes are significantly damaged and only a few immature myotubes were formed [73]. As glutathione peroxidase -1 (GPX1) is a highly conserved antioxidant that reduces two ROSs (hydrogen peroxide and hydroperoxides), this result indicated that ROS are actively involved in controlling muscle differentiation and play a key role during muscle regeneration and repair.

In mature skeletal muscle cells, nNOS are mainly localized to specific domains of the cell membrane, expressing on both skeletal muscle type I (slow twitch) and type II (fast twitch). Immunohistochemical studies confirmed that the expression levels of nNOS in these two types of muscle fibers are almost same [71], while Frandsen et al. [74] pointed out that the expression level of type I muscle fibers in cytoplasm and membrane of human vastus lateralis is higher than type II fibers. nNOS is considered as the main source of NO in human muscles such as gastrocnemius and quadriceps muscles. nNOS is constitutively expressed and its expression is increased by crush injury, muscle activity and ageing [37].

C: Development of MyoNovin

This chapter is a treatise on the major features of the skeletal muscle regenerator – MyoNovin (1-(3,4-Bis-nitrooxy-butoxy)-2-methoxy-benzene). The structure of MyoNovin and the selected base compound, guaifenesin and isosorbide dinitrate (ISDN), are shown in Figure 3.

Wang et al. introduced the synthesis of MyoNovin using 2-methoxy-phenol (guaiacol) as starting material [75]. Treatment of 2-methoxy-phenol with allyl bromide under the presence of potassium carbonate gave the immediate precursor 1-allyloxy-2-methoxy-benzene. Subsequent treatment of 1-allyloxy-2-methoxy-benzene with iodine under the promotion of silver nitrate formed an iodinium ion. The iodinium ion is opened via S_N2 reaction by nitrate (or silver nitrate) to give the first intermediate, the iodo-nitrate. The iodine is displaced via another S_N2 reaction resulted in the formation of MyoNovin as shown in Figure 4.

As a NO-donor, MyoNovin maintains the ability of delivering nitric oxide to activate satellite cells. From a structural point of view, the two-nitro groups on MyoNovin are the functional sites, as these functional sites are responsible for carrying nitric oxide. Based on the structure, for one MyoNovin molecule two molecules of nitric oxide will be delivered to the satellite cells. This likely results result in an increase in muscle satellite cell activation and proliferation in a similar manner as with isosorbide dinitrate [76]. Thus, MyoNovin's major

Figure 3. The structure of MyoNovin and the selected base compound, guaifenesin and isosorbide dinitrate (ISDN).

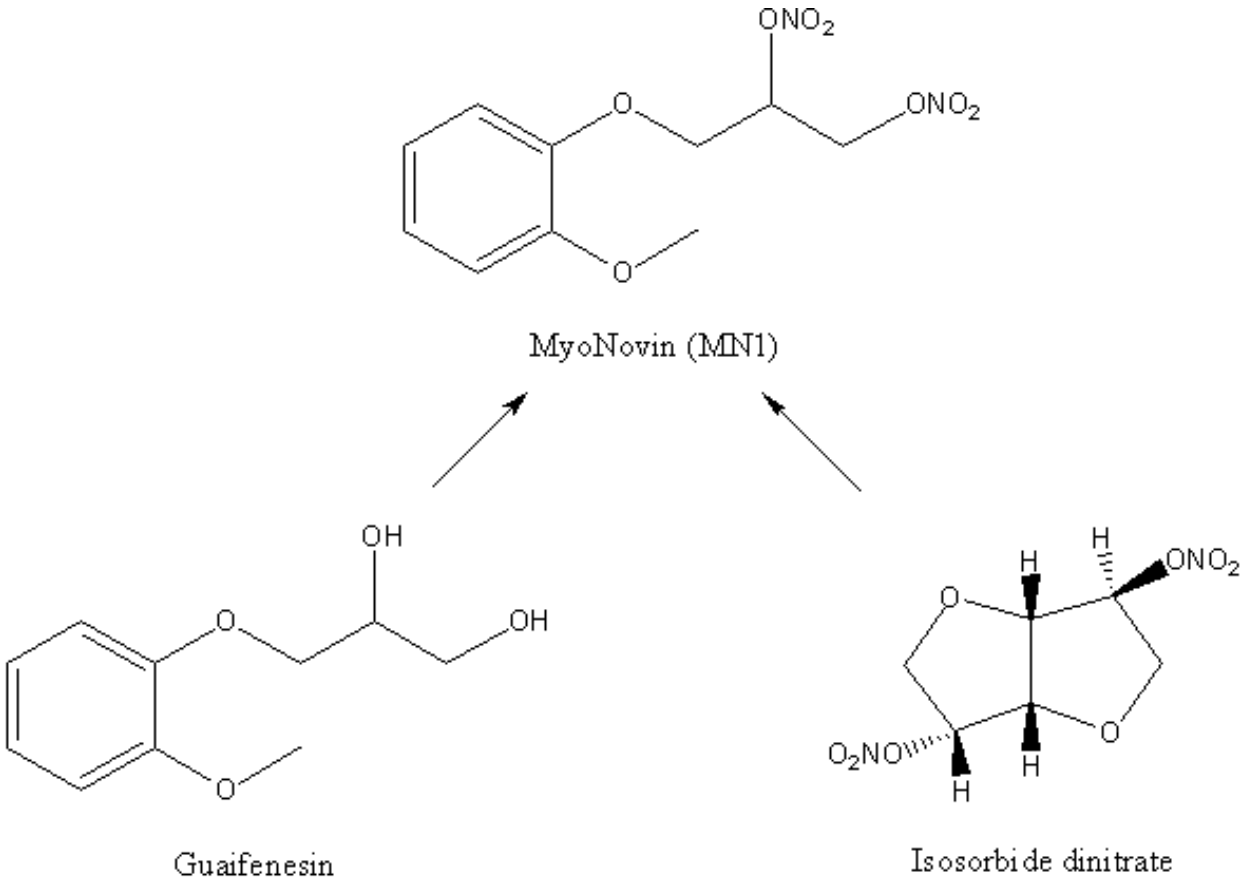

function in the muscle is to release nitric oxide to activate satellite cells.

In order to test the theory, Wang et al. (2009) first tested the nitric oxide production from MyoNovin in muscle and liver homogenates [75]. He characterized a triplet-NO complex generated by $Fe^{2+}(MGD)_2$ trap and nitric oxide using electron paramagnetic resonance (EPR) spectroscopy. The result was encouraging. Negative controls (liver homogenate without guaifensin dinitrate), back muscle homogenate with MyoNovin, liver homogenate with MyoNovin and positive control (liver homogenate and NO gas) were tested in the experiment. All test groups and the positive control showed similar unique triplet spectrums ranged from 3225 to 3312.5 gauss. In the EPR experiments, MyoNovin was confirmed to increase nitric oxide release.

The time course of nitric oxide release was determined by plotting the EPR signal over time following the addition of MyoNovin [75]. The result showed most of nitric oxide was released between 1 and 2 hrs followed by a gradually decline of nitric oxide.

Figure 4. MyoNovin synthesis.

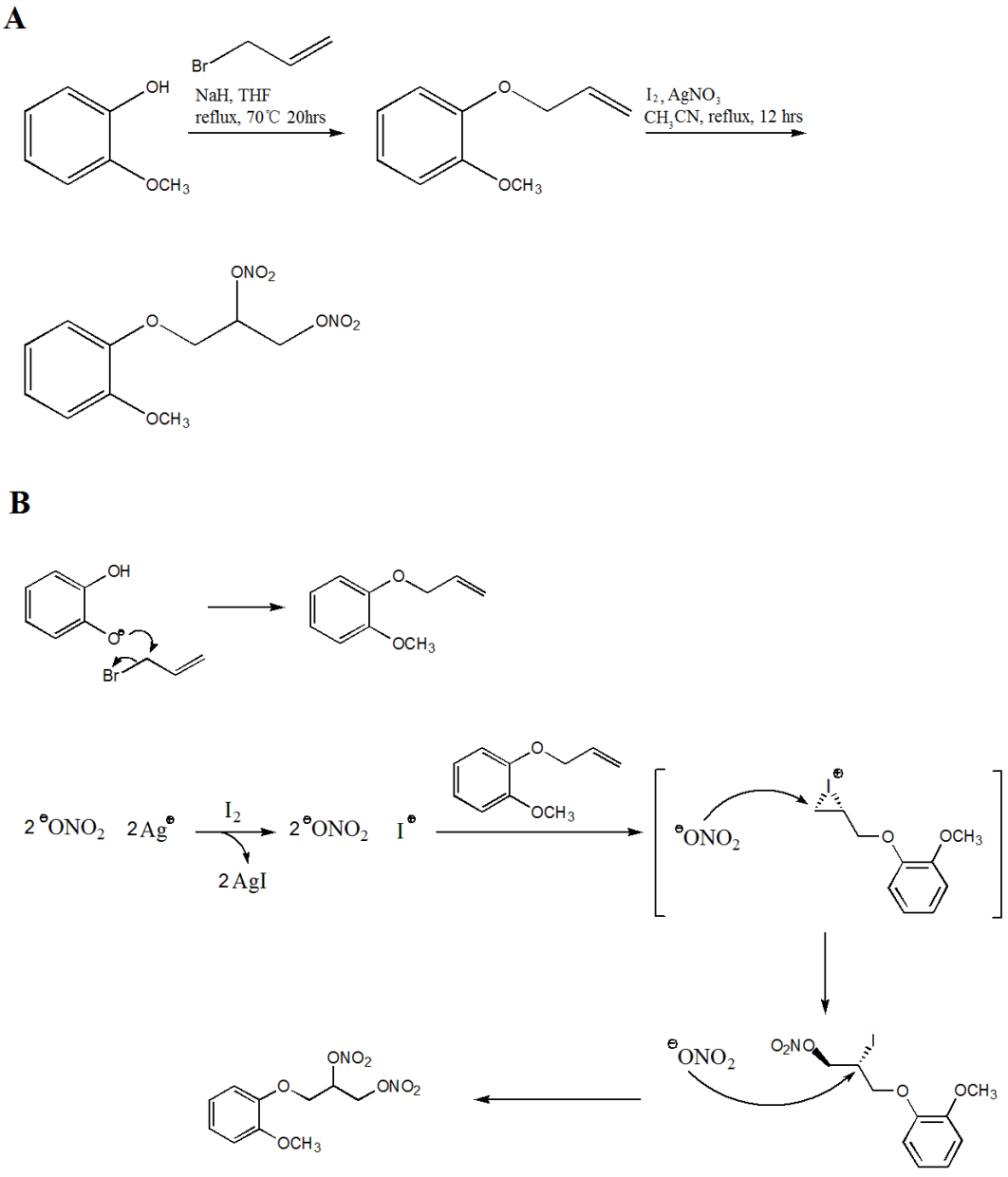

Wang et al. went on the test a transdermal treatment of MyoNovin to show its *in vivo* bioactivity [75]. Its ability to increase DNA synthesis in skeletal muscles was first tested. Adult mice were treated with MyoNovin (2%) ointment on the back skin for 24 hours. No adverse effects were noted during the treatment interval. MyoNovin showed a 37% and 39% increase in DNA synthesis in both back muscle and quadriceps muscle, respectively compared to the control group. MyoNovin's activity in enhancing DNA synthesis activity was similar when compared to the positive control ISDN, which suggested that MyoNovin has a strong ability in promoting muscle regeneration.

Finally, MyoNovin was shown to activate satellite cells *in vivo* [75]. Mice treated with MyoNovin were chosen as the animal model and Myf-5 was chosen as the maker to analyze the amount of satellite cells. After 24 hours Myf-5 showed a dramatic increase in back muscle and quadriceps muscle of 40% and 55%，respectively compared to the control group. These results indicated that satellite cells were activated by MyoNovin in about 24 hours, which means MyoNovin successfully released nitric oxide and affected the regeneration process.

D: Solubility Enhancement Techniques

Drug candidates are often very lipophilic when selected from combinatorial chemistry

research and/or biologically based high-throughput screening. It is estimated that approximate 40% of new chemical entities, which possess promising pharmacological activity, have poor water-solubility [76]. Unfortunately this often poses a significant barrier in pharmaceutical formulation development by limiting acceptable bioavailability.

Solubility is a chemical property referring to the ability for solid, liquid, or gaseous chemical substances (the solute) to dissolve in a solid, liquid, or gaseous solvent. The resulting homogeneous solution can be measured in terms of the maximum amount of solute dissolved in a solvent at equilibrium. The solubility of a substance is determined by the substance itself and on external conditions such as temperature and pressure. The World Health Organization (WHO） pharmacopoeia library describes different solubility levels (Table 1). The partition coefficient (Log P) is a ratio of between the solubility of an unionized compound in a hydrophobic solvent (octanol) and a hydrophilic solvent (water). Log P measurements are useful parameters in understanding the behavior of drug molecules in liquids. The Biopharmaceutics Classification System (BCS) was set up for predicting intestinal drug absorption. BCS relates the drug's chemical property (solubility) to bioavailability. BCS divides drug substances into four classes as judged by permeability and solubility: class I— highly soluble and highly permeable, class II— poorly soluble and highly permeable, class III— poorly soluble and highly permeable and class IV— poorly soluble and poorly permeable. BCS indicates that class II and class IV drugs have

low solubility, which becomes the rate-limiting step for oral absorption. Drugs in these classes are associated with limited or poor bioavailability. Oral administration is the most commonly used drug delivery system mainly because of its convenient route of administration, high patient compliance, cost effectiveness, and formulation design flexibility. Thus, oral drug products become the first choice for the formulation of many new chemical entities. Solubility plays an important role in the absorption of drugs from oral dosage forms. However, it must be kept in mind that a poorly soluble chemical entity may also be associated with good bioavailability, resulting in acceptable plasma drug concentrations for therapeutic purposes.

Table 1 The level of solubility provided by WHO pharmacopoeia library.

Description	Approx. Volume (ml) of Solvent Needed to Dissolve 1g of Solute	Examples of Drugs
Very Soluble	Less than 1	Metoprolol
Freely Soluble	1 to 10	Ipratropium bromide
Soluble	10 to 30	Propananolol
Sparingly Soluble	30 to 100	Quinidine Sulphate
Slightly Soluble	100 to 1000	Fludrabine
Very Slightly Soluble	1000 to 10,000	Doxazocine
Practically Insoluble	Greater than 10,000	Chlorambucil

Factors affecting bioavailability include dosage form and physiological factors. Dosage form factors include the molecule's water solubility, pKa, as well as the excipients that go into the tablet that may affect disintegration time and dissolution rate. Physiological factors include gastric content constituents, motility, surface area, transporters, blood flow, metabolic enzymes, and disease state. The most frequent causes of low oral bioavailability are poor solubility and permeability. Orally administered drugs are absorbed by the enterocytes of the small intestine and pass into the mesenteric and portal circulation leading to the liver. Thus, metabolism may occur in advance of the drug reaching the systemic circulation. Poorly water-soluble drugs or those highly metabolized often require higher dosages than water-soluble drugs for equivalent plasma concentrations to be obtained resulting in bulkier tablets and possibly higher adverse effects.

In cell culture experiments, how much lipophilic drug dissolves in aqueous medium and how well the drug is absorbed by cells are two key determinants of bioactivity. Thus, the choice of solvent is important. Dimethyl sulfoxide (DMSO) is a dipolar, aprotic solvent that has a strong affinity for cell membrane. It is widely believed that DMSO, as a cell culture reagent, helps lipid-soluble drugs traverse the cell membrane to promote drug absorption. However, there is direct evidence to support the concept that DMSO shows cytotoxicity at certain concentrations. Results from colonic epithelial cells investigation on DMSO have provided good evidence for

inducing significant apoptosis at concentrations of 2% [77]. Studies with SV40-transformed human keratinocytes also showed that DNA damage resulted following treatment with 2.5% DMSO [78]. Collectively, the current literature reveals that cytotoxicity of DMSO exists at a very low concentration and the sensitivity in different tissues may be differential. To enhance the accuracy of the outcome and reduce adverse effects, the ideal condition was to replace DMSO with water or reduce the amount of DMSO as much as possible. Therefore, improving the water solubility of MyoNovin is extremely important.

There are many methods available to increase the solubility of molecules; these include particle size reduction, solid-dispersion, and salt formation. All methods are associated with both positive and negative attributes. Class II (low solubility and high permeability) substances have solubility as the rate limiting step in the overall bioavailability process. Increasing the water solubility and enhancing the dissolution rate of the drug may result in enhancement of bioavailability. However, the BCS class IV drugs are always associated with poor bioavailability because both solubility and absorption through the intestinal mucosa is poor. This situation makes the need for these drugs to be administered in high-doses [79]. Chemical modifications to BCS class IV drugs with the intent of enhancing water solubility may prove to be productive.

1. Techniques for improvement in drug solubilization

Solubility improvement techniques can be general divided into three categories：physical modification or chemical modification of the drug substance, and miscellaneous techniques. Physical modifications include but are not limited to particle size reduction and changes in pH of the solvent system. Chemical modification includes solvent pH adjustment and structural modification (applying a solvent pH change for oral and parenteral drug, salt formation, prodrug strategy and introducing hydrophilic group, modification of pKa and etc.). Miscellaneous modifications methods include the use of adjuvants (surfactants).

The solubility of a solid drug is related to the drug's particle size [80]. For soluble drugs, particle size has little effect on solubility but for poorly soluble drugs smaller particles result in higher surface area, which increases the interaction with the solvent resulting in enhanced solubility. When the particle radius is larger than 2 microns, particle size has little effect on solubility, however, when particle size is between 0.1 to 100 nm, solubility increases with decreasing particle size [81]. Therefore, reducing particle size is an effective method to improve the solubility of poorly soluble drugs. Methods of particle size reduction include jet milling, spray drying and super critical fluid technology.

Water insoluble drugs may potentially dissolve in water by altering the pH. Thus, changes

in the solvent pH become the simplest and most economic way to increase drug solubility. Buffer characteristics and stability of the drug to the selected pH are important parameters to be considered. For weakly acidic drugs, higher pH is required for ionization and enhanced solubility. Alterations in pH also can be combined with other techniques such as complexation, micelle formation and co-solvency to enhance solubility.

Salt formation is important for dissociation and hence ionization of acidic or basic drugs. Salts of acidic and basic drugs always have higher solubility than their corresponding acid or base forms. Sulfadiazine, for example, is an antitoxoplasmosis drug with its mechanism of action being the stopping of production of folate inside the bacterial cell. The solubility of sulfadiazine in water at 25℃ is 0.0002 M [82]. However, the sodium salt form of sulfadiazine enhances the solubility to 1.9207 M [83] and makes it more practical to use as a drug. Salt formation is the most popular method to increase aqueous drug solubility for parenteral administration [84]. Sodium and potassium salts are the most common choice for weak acids, while for weakly basic drugs or strong acids, salts are prepared using hydrochloride or sulphate salts.

Prodrugs are inert drug precursors that are metabolized to pharmacologically active moieties. Prodrugs can also be the combination of two pharmacologically active molecules. There are several factors worth considering when designing a prodrug that include defining which functional group may be modified in the parent drug. The introduction of the modified

group should be safe and effectively removed *in vivo*. Selection of the modifying group should also consider disease conditions and required dosage. The biopharmaceutics, pharmacokinetics, and toxicology characteristics of both prodrug and active drug need to be fully understood. Commonly modified functional groups in prodrug design are carboxyl, hydroxyl, amino, phosphate / phosphoric acid ester, carbonyl group. Other functional groups include esters, carbonates, carbamates, amides, phosphates, and oxime. Many water-soluble prodrugs were created though the addition of an ionizable group (such as phosphate groups) to the parent drug molecule to improve solubility. Fosamprenavir is the phosphate prodrug of HIV protease inhibitors amprenavir. The solubility and oral bioavailability of Fosamprenavir has been improved compared to amprenavir [85].

Introduction of hydrophilic groups into a molecule will generally increase its solubility in water. Hydrophilic groups include sodium sulfate ($-SO_3Na$), carboxylate (-COONa), alcohol (-OH), amino ($-NH_2$), and polyhydric alcohol or sugar groups. For example, Vitamin K3 (menadione) is insoluble in water, however, the introduction of sodium bisulfite ($-SO_3HNa$), menadione sodium bisulfite, increases the solubility two-fold. Introducing some hydrophilic groups to the parent drug may however have deleterious effects on the drug's pharmacological activity.

In the present work MyoNovin was chemically modified to enhance its water solubility. The

main reason why a technique like salt or prodrug formation will not work for MyoNovin is the molecule contains no ionizable functional group. The addition of a charged group onto the molecule would permit salt formation and enhancement of solubility. Another strategy for enhancing water solubility would be to chemically introduce a hydrophilic group onto the molecule although it is recognized that such changes may alter the bioactivity of MyoNovin.

Some screening rules were noted when potential groups were selected. Log P was the first parameter in our research. Philip J.Hajduk reported a statistical analysis of the different potency of common chemical substituents against 30 different protein targets [86]. Molecules with low Log P values were associated with greater solubility. Based on this rule, eight different functional groups that have Log P values lower than MyoNovin's methoxy group were found so the methoxy group was the functional group chosen to be replaced. Three novel structures were selected based on the prodrug strategy and the degree of difficulty in synthesis. These included methanesulfonic (MN2), carboxyl group (MN3), and an acetamide (MN4). Figure 5 is shown the structure of MyoNovin (MN1) and three new analogs. Among them, the carboxyl group has a similar Log P value to the methoxy group. The rationale for choosing to replace this group was that the molecule could be easily further modified into a salt or a pro-prodrug form to increase the solubility of the new drug molecule.

Figure 5 Four structures of modified MyoNovin analogs

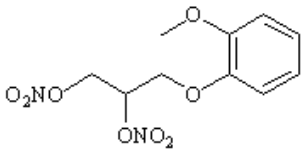

1-(2,3-Bis-nitrooxy-propoxy)-2-methoxy-benzene

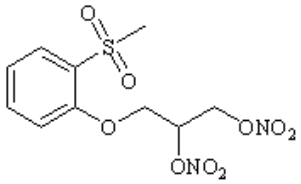

1-(2,3-Bis-nitrooxy-propoxy)-2-methanesulfonyl-benzene

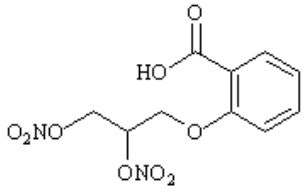

2-(2,3-Bis-nitrooxy-propoxy)-benzoic acid

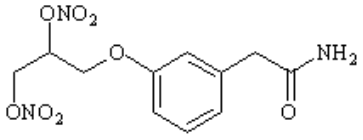

2-[3-(2,3-Bis-nitrooxy-propoxy)-phenyl]-acetamide

E: Solubility Measurement

The water solubility of a compound is the compound's dispersion characteristics in an aqueous media, and typically is represented by the saturation concentration in water. The process is in a dynamic equilibrium. Several measurement methods are available for studying the aqueous solubility of organic chemicals. Kinetic and thermodynamic methods are used most frequently. The thermodynamic method often uses the classic shake-flask method and this method is widely applied in the field of drug research. The process of determining the

equilibrium solubility includes several essential steps; (1) place an excess of solid solute in the liquid solvent; (2) seal and hold at the temperature of interest for few days to weeks; (3) during this period, agitate continuously or intermittently in order to promote dissolution; (4) after standing, the upper saturated supernatant is analyzed by means of suitable analytical method(s) to obtain the solubility data of the compound in the liquid solvent. The data measured by the kinetic method is dependent on the operating time and the degree of supersaturation, and is often larger than the value measured by the equilibrium method. Its important to note that the experimental data obtained from different kinetic experimental devices are inconsistent. The establishment of the solubility study in this investigation was based on both the thermodynamic and kinetic methods. Details of these methods are discussed below.

1. Equilibrium method

Despite a large number of new solubility measurement methods being developed, the thermodynamic method is still recognized as the standard method for verifying other solubility measurements. The shake flask method is the traditional way to determine equilibrium solubility for a given a specific pH and temperature. Based on this method, an excess of compound is added to a defined medium and usually shaken for 24h or longer before testing. Heating the solvent and excess solute and then cooling it down and confirming the presence of un-dissolved

solute can make saturated solutions. After filtration, the amount of compound contained in the sample is usually determined by ultraviolet/visible spectroscopy or chromatographic methods. Since the operational details of the thermodynamic method are not precisely defined, the thermodynamic method does not have a universal standard procedure. During solubility measurements, very different operating conditions are applied. In practical terms, mixing time records from 24 hours to two weeks, standing time is usually from 24 hours to 3 days, and different solid-liquid separation techniques are used such as sedimentation, centrifugation, or filtration. In 2008, E.Bake [87] demonstrated that experimental conditions (including temperature, sedimentation time, composition of aqueous buffer) strongly affect results when measuring hydrochlorothiazide by the classic shake-flask method. They proposed a new protocol that reduces the stirring time from 48 hours to 6 hours, which greatly reduces the time for completion of the study.

2. Kinetic method

In the initial stages of drug development, the need for screening a large number of drugs needs to be taken into account. Since the thermodynamic method is time consuming, a kinetic method based on detecting the emergence of precipitate in an aqueous solution was established to overcome the problem. The kinetic method was first used in the drug solubility determination

in 1997 by Lipinski [88]. The basic principle involves the use of DMSO as a co-solvent. DMSO can change the dielectric constant of the solution, making the solvent better able to dissolve more lipophilic compounds. Test compounds are prepared using 1% DMSO solution. A small amount of DMSO stock is first added to the aqueous solution or buffer solution until it reaches the upper limit of 1%. The concentration at which the precipitate starts to appear is detected by an optical method and is considered as the kinetic solubility result. In recent years, the dilution process and the detection methods for kinetic measurements have been modified and improved. With increasing concentration of test substance, the amount of DMSO added will increase correspondingly, which may lead to a higher UV absorption due to the high UV cutoff of 268 nm for DMSO and an unreliable kinetic solubility result. Therefore, some of the investigations [89,90] use glyme (dimethoxyethane) or ethanol as cosolvents since these have much lower UV absorption cutoffs at 210 and 220 nm respectively. However, this still cannot always provide a reliable result for the compounds solubility and may affect other properties of the test compounds such as the cellular permeability. For these reasons, the type of co-solvent and its concentration in aqueous solution are reported in the literature. In this study, acetone was used to initially dissolve the test compounds but it was not operating as a co-solvent. The role of acetone was to dissolve the test compounds and allow them to be dispensed proportionately to each well. By doing that, each well contained an appropriate amount of test compound. The acetone was

evaporated before any aqueous vehicle was added to the wells so that the acetone was not a cosolvent in the solubility determination. Prior to adding water in each well, the absorbance at 630 nm was recorded twice to ensure that the acetone had all evaporated.

Kinetic measurement methods are mainly divided into two categories. One is measuring the concentration of the solution once precipitate had been removed; the other uses the precipitated compound as the indicator of the concentration limit [91-93]. The basic principle of the second method is due to the fact that particles block light from reaching the detector, so the appearance of a precipitate was indirectly tested by the decreased light intensity while increasing the ultraviolet absorption of solution. T.A. Fligge [94] and his colleges measured the kinetic solubility of 9,000 drugs tested by a nephelometer with a laser light source focusing to 1.9 mm. A similar principle was used in the present studies. Appearance of turbidity from four similar compounds was measured by light scattering at 630 nm. The measurement time for samples from a 96-well black plate can be decreased to 60 seconds. The time advantage of this approach makes it a good choice for solubility measurements particularly in drug discovery at the early stage due to the relatively smaller quantities of drug required. This method is particularly suitable for drug screening.

3. Other methods

3.1 Potentiometric method

Avdeef [95] first used potentiometric methods in the determination of solubility, which is suitable for measuring the solubility of ionic compounds and the corresponding solubility-pH curve. The theoretical basis of this method is to find a mutant point where substances dissolve in titration mixture of titration curve and reach saturation. This mutant point is used to calculate reactant concentrations in saturated solutions of ionizable compounds.

Potentiometric titration is primarily divided into pSvol Gemini method [96] and Cheqsol method [97], both of which have been commercialized. These two methods differ in total experiment time required to completion and titration processes. Avdeef et al. [98] measured solubility-pH curves for twelve compounds and reported that they differ in six orders of magnitude. In their paper, solubility of test substances was measured by potentiometric titration and shake-flask method. Two hundred twelve separate results measured by classic shake-flask method and 65 results measured by potentiometric titration had good matches. The authors considered pSvol Gemini method as being very economical because only 100 mg of sample is consumed in each experiment. This method was endorsed by FDA as appropriate to measure the solubility for the Biopharmaceutics Classification System.

Stuart et al. [99] proposed a simplified pSvol Gemini method, which can reduce the measurement time. This method requires changing the concentration of the neutral substances through the addition of hydrochloric acid or potassium hydroxide solution, followed by measuring the pH change resulting from dissolution or precipitation. Solubility-pH curves cannot be obtained directly from this method but must be calculated through the Henderson–Hasselbach equation. This method can measure the equilibrium solubility, kinetic solubility and intrinsic solubility within 20 ~ 80 min. However, it is not applicable for compounds that undergo agglomeration.

3.2 Latest Development of Equilibrium Measurement and Kinetic Measurement

In recent years, a series of new methods used to measure drug solubility have been proposed and have advantages such as fast measurement time, easy storage tested compounds and a higher level of automation. These new methods can be theoretically divided into two types: one is to prolong the equilibrium time of the already formed kinetic solubility measurement method; the other is to measure with the solid compound formed after drying the solvent- DMSO [100]. The first method is mainly used to prolong the balance time needed, when adding raw liquid material

to water in the kinetic solubility measurement process, from several seconds or several minutes to several hours and even several days. This means that a long equilibrium time allows the kinetic solubility value to approach the equilibrium solubility value slowly. K. A. Dehring et al. [92] studied the solubility of 124 compounds, finding that the solubility of only 2.3% compounds decreased within 24 h. But this comparison result is based on comparing the results measured by semi-automatic equilibrium solubility measurement methods, and the property of sediment matters is not characterized. K. Sugano et al. [100]measured the solubility of 26 compounds, finding that the solubility of more than 50% of the compounds showed a significant decrease in solubility along with the increase in time needed to reach equilibrium. A very large difference is shown in the results of above researchers, which may be explained by the final DMSO concentration, the nature of molecules, the purity of test compounds, and the composition of the buffer solution [101]. As suggested in the above findings, these results have similar result with thermal equilibrium solubility along with the prolonged time.

The second new method uses DMSO at the beginning of the experiment, but this solvent is removed by evaporation before any solubility measurements are made, and the following operational procedures are the same as the kinetic solubility measurement method. The measurement method is based on the lyophilized solubility assay (LYSA). LYSA often needs to consider the nature of the solid and limitations of impurities. This approach has two advantages:

1) solid powders are prepared into standard raw material solution, allowing the sample to be dispersed well; 2) solid materials are used for measurement. Thus, hundreds of compounds could be measured per week, and the few amount of test compound are needed.

II. Hypothesis and Objectives

Hypothesis

Reports indicate that nitric oxide released from muscle fibers mediates satellite cell activation [46,60]. Based on these reports the development of a NO-based compound to target NO delivery to skeletal muscle was reported [75]. However, the nitric oxide releasing drug MyoNovin is poorly water-soluble. In order to study the bioactivity of MyoNovin, it must first be dissolved in DMSO, which necessitates appropriate controls that include DMSO. Enhancing the water solubility of MyoNovin will allow for easier dosing in both *in vitro* and *in vivo* studies. Whether improved biological activity is seen with the enhanced water solubility is not known. Thus, the null hypothesis to be tested is enhancing the water solubility of MyoNovin will not improve the biological activity of the drug when administered on a molar basis using *in vitro* cell culture studies.

Objective

The main objective of this research project is to enhance the water solubility of MyoNovin. The specific aims of this work were to: 1) to design, synthesize and purify MyoNovin and novel water soluble MyoNovin analogues and; 2) to evaluate the bioactivity of the novel MyoNovin

analogues and compare them to MyoNovin.

III. Materials and Methods

A. **Materials**

All chemicals were purchased from Sigma-Aldrich Canada Ltd. (Oakville, ON) unless otherwise stated. Aldrich 288624 silica gel was used for all chromatography. Preparative thin layer chromatography was carried out on aluminum baked TLC plate precoated with SiliaFlash® silica gel (2 mm thickness). All organic solutions were dried over anhydrous sodium carbonate.

B. Methods

1. Chemical Synthesis

1.1 Synthesis procedure for MyoNovin (MN1)

Figure 6 Synthesis procedure for MyoNovin (MN1)

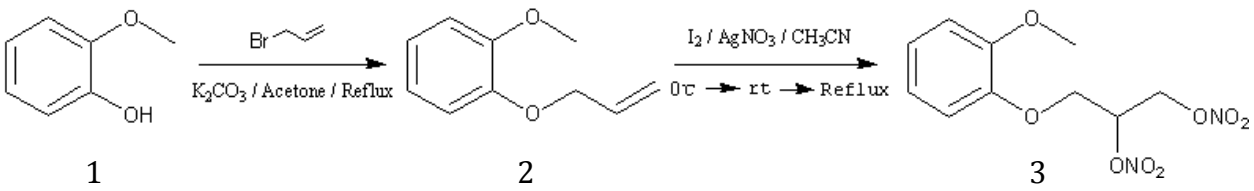

1 2 3

Allyloxy-2-methoxy-benzene (2)

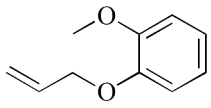

A schematic of the synthesis of 2 is shown in Figure 6. To a stirred suspension of 2-methoxy-phenol (1.24 g, 0.01 mol) in dry acetone (20 ml) allyl bromide (1.45 g, 0.012 mol) and potassium carbonate (1.50 g, 0.015 mol) were added. The reaction mixture was heated at 70℃ overnight. The resulting solution was cooled to room temperature and filtered through a sintered glass funnel to remove any solid residue. The filtrate was evaporated to dryness to obtain compound 2 (1.51 g) as a colorless liquid. Yield=~92%

1-(3,4-Bis-nitrooxy-butoxy)-2-methoxy-benzene (3)

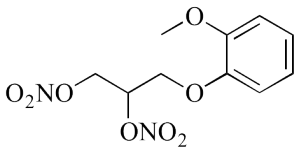

A schematic of the synthesis of 3 is shown in Figure 6. To an ice cooled, stirred solution of compound 2 (1.0 g; 6.09 mmol) in acetonitrile (12 ml) silver nitrate (4.138 g; 0.024 mol) was added. The reaction mixture was cooled in an ice bath with stirring and iodine (1.56 g) was added. After the iodine had dissolved, the reaction mixture was refluxed for 12 hrs, filtered, poured into water and extracted with ethyl acetate. The organic layer was washed with brine, dried, and evaporated. The oil thus obtained was purified by flash chromatography (eluent from hexanes/EtOAc 10/1 to 3/1 v/v) to isolate compound 3 (1.24 g) as a yellowish semisolid. Yield=70.7%. NMR results yielded: ^{1}H NMR ($CDCl_3$): δ 3.90 (s, 3H), 4.58 (d, 2H, J = 5.1Hz), 5.28 (dd, 1H, J = 6.5Hz, J = 12.8Hz), 5.42 (dd, 1H, J = 3.3Hz, J = 12.9Hz), 6.05-6.18 (m, 1H), 6.89-6.97 (m, 4H); ^{13}C NMR ($CDCl_3$): δ 55.7 (CH_3), 67.1 (CH_2), 69.0 (CH_2), 76.7~77.2 (CH), 112.4 (CH), 116.8 (CH), 121.0 (CH), 123.7 (CH), 147.1 (CO), 150.4 (CO).

1.2 Synthesis procedure for MyoNovin Analog 1 (MN2)

Figure 7 Synthesis procedure for MyoNovin Analog 1 (MN2)

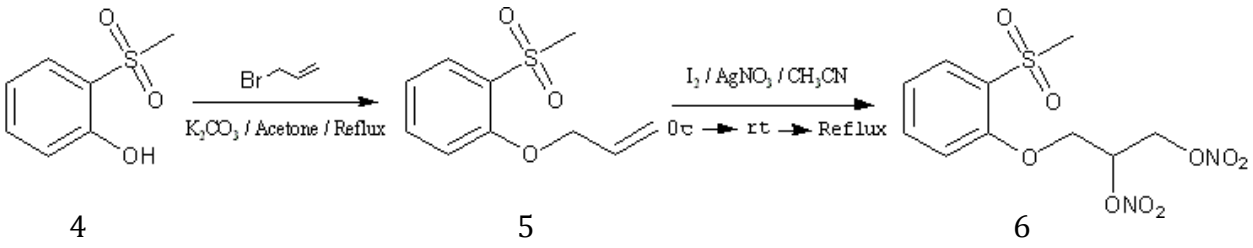

4 5 6

1-Allyloxy-2-methanesulfonyl-benzene (5)

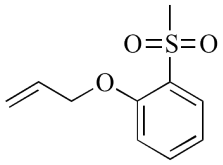

A schematic of the synthesis of 5 is shown in Figure 7. To a stirred suspension of 2-methanesulfonyl-phenol (0.1g, 0.58 mmol) in dry acetone (2 ml) allyl bromide (0.084 g, 0.69 mmol) and potassium carbonate (0.087 g, 0.87 mmol) were added. The reaction mixture was heated at 70℃ overnight. The resulting solution was cooled to room temperature and filtered through a sintered funnel to remove solid residue. The filtrate was evaporated to dryness to obtain compound 5 (0.11 g) as a colorless liquid. Yield=89.4%

1-(2,3-Bis-nitrooxy-propoxy)-2-methanesulfonyl-benzene (6)

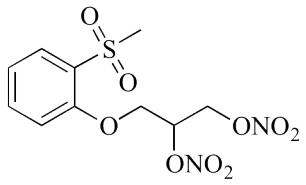

A schematic of the synthesis of 6 is shown in Figure 7. To an ice cooled, stirred solution of compound 5 (0.1 g; 0.47 mmol) in acetonitrile (2 ml) silver nitrate (0.32 g; 1.88 mmol) was added. The reaction mixture was cooled in an ice bath with stirring followed by the addition of iodine (0.18 g). After the iodine had dissolved, the reaction mixture was refluxed for 12 hrs, filtered, poured into water and extracted with ethyl acetate. The organic layer was washed with brine, dried, and evaporated. The oil obtained was purified by flash chromatography (eluent from hexanes/EtOAc 10/1 to 3/1 v/v) to isolate compound 6 (0.114 g) as colorless sticky liquid. Yield=72.3%. NMR results yielded: ^{1}H NMR ($CDCl_3$): δ 3.21 (s, 3H), 4.46 (d, 2H, J = 5.0Hz), 4.94 (dd, 1H, J = 6.3Hz, J = 13.0Hz), 5.06 (dd, 1H, J = 3.5Hz, J = 12.9Hz), 5.68-5.71 (m, 1H), 7.05 (d, 1H, J = 8.4Hz), 7.24 (d, 1H, J = 8.1Hz), 7.65 (td, 1H, J = 1.7Hz, J = 8.6Hz), 8.03 (dd, 1H, J = 1.6Hz, J = 7.8Hz); ^{13}C NMR ($CDCl_3$): δ 43.2 (CH_3), 66.3 (CH_2), 68.7 (CH_2), 76.4 (CH), 113.7 (CH), 122.6 (CH), 129.4 (CH), 130.3 (CH), 135.7 (CS), 157.4 (CO), 155.2 (CO).

1.3 Synthesis procedure for MyoNovin Analog 2 (MN3)

Figure 8 Synthesis procedure for MyoNovin Analog 2 (MN3)

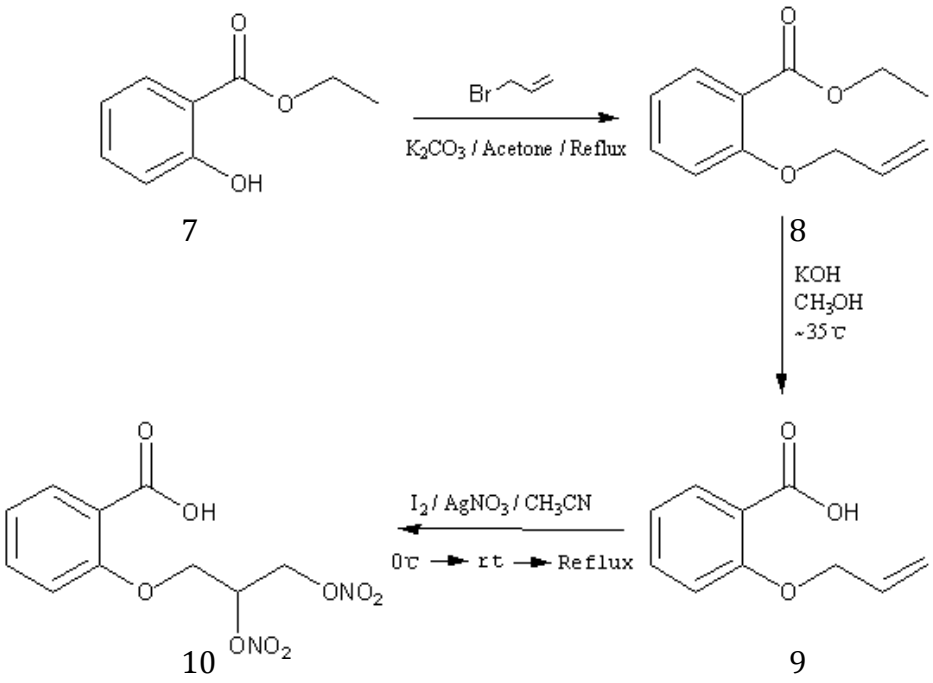

2-Allyloxy-benzoic acid ethyl ester (8)

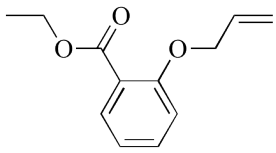

A schematic of the synthesis of 8 is shown in Figure 8. To a stirred suspension of ethyl 2-hydroxybenzoate (5 g; 30.08 mmol) in dry acetone (20 ml) allyl bromide (3.124 ml, 36.09 mmol) and potassium carbonate (4.52 g, 45.12 mmol) were added. The reaction mixture was heated at 65℃ overnight. The resulting solution was cooled to room temperature and filtered through a sintered funnel to remove solid residue. The filtrate was evaporated to dryness to

obtain compound 8 (6.75 g) as a colorless liquid and used for next reaction without further purification. Yield=108.8%

2-Allyloxy-benzoic acid (9)

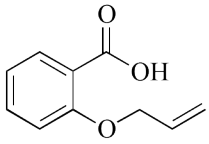

A schematic of the synthesis of 9 is shown in Figure 8. To a suspension of compound 8 (2.5 g; 12.13 mmol) in methanol (12 ml), was added KOH (1.357 g). The reaction mixture was maintained at ~35℃ for two hours. The reaction was quenched by addition of 10 ml water. The reaction was extracted with ether (2x5 ml) and the aqueous portion was acidified to pH=2 with 6N hydrochloric acid and extracted with ether (3x5 ml). The combined ether extracts were dried with Na_2SO_4 and concentrated to get 9 (2.24 g) as a white solid and used for next reaction without further purification. Yield: 103.7%

2-(3,4-Bis-nitrooxy-butoxy)-benzoic acid (10)

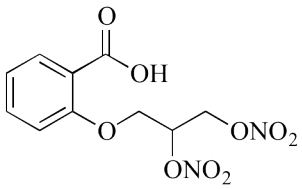

A schematic of the synthesis of 10 is shown in Figure 8. To an ice cooled, stirred solution of compound 9 (2.24 g; 0.0126 mol) in acetonitrile (45 ml) silver nitrate (8.56 g; 0.0506 mol) was

added. The reaction mixture was cooled in ice bath with stirring and iodine (4.31 g) was added. After the iodine had dissolved, the reaction mixture was refluxed for 12 hrs, filtered, poured into water and extracted with ethyl acetate. The organic layer was washed with brine, dried, and evaporated. The oil thus obtained was purified by flash chromatography (eluent from hexanes/EtOAc 10/1 to 3/1 v/v) to isolate compound 10 (2.93 g). Yield was 73.5%. NMR results yielded: ^{1}H NMR ($CDCl_3$): δ 4.42 (d, 2H, J = 8.0Hz), 4.91 (dd, 1H, J = 6.21Hz, J = 12.9Hz), 5.04 (dd, 1H, J = 3.63Hz, J = 12.9Hz), 5.69-5.72 (m, 1H), 7.00 (d, 1H, J = 8.4Hz), 7.17 (td, 1H, J = 0.8Hz, J = 8.3Hz), 7.59 (td, 1H, J = 1.7Hz, J = 8.5Hz), 8.06 (d, 1H, J = 8.52Hz); ^{13}C NMR ($CDCl_3$): δ 66.1 (CH_2), 68.7 (CH_2), 76.4 (CH), 113.6 (CH), 118.9 (C), 122.5 (CH), 133.5 (CH), 134.9 (CH), 157.4 (CO), 167.6 (COOH).

1.4 Synthesis procedure for MyoNovin Analog 3 (MN4)

Figure 9 Synthesis procedure for MyoNovin Analog 3 (MN4)

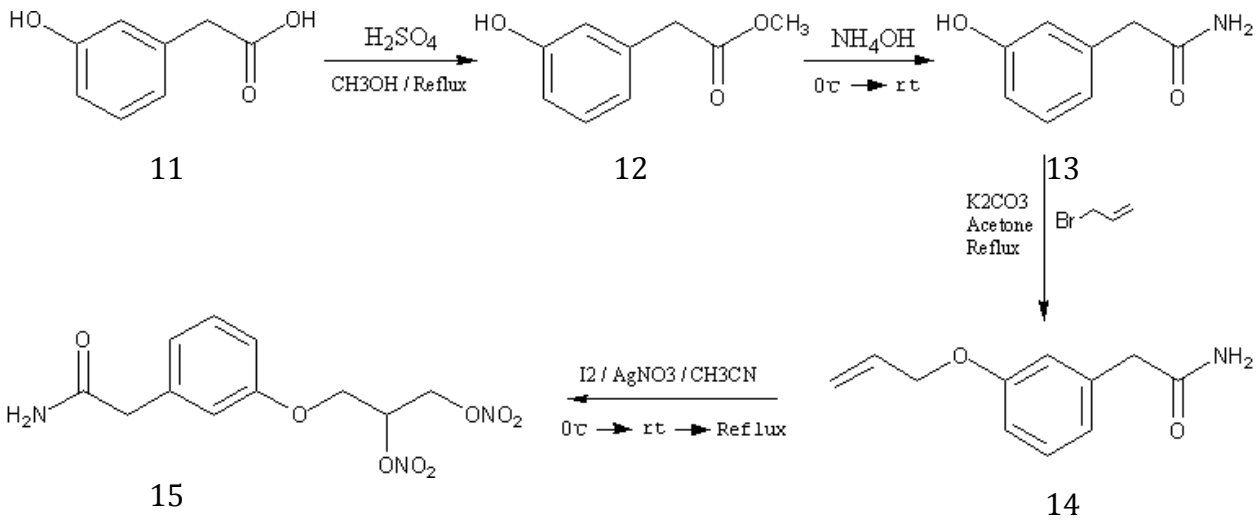

(3-hydroxyphenyl) acetone (12)

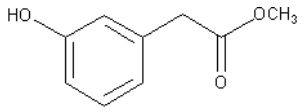

A schematic of the synthesis of 12 is shown in Figure 9. To a stirred suspension of (3-hydroxy-phenyl)-acetic acid (2 g, 13.2 mmol) in methanol (24 ml) concentrated sulphuric acid (2 ml) was added. The reaction mixture was heated to reflux for 5 hours. The resulting solution was cooled to room temperature and evaporated. The residue was dissolved in CH_2Cl_2 (24 ml) and washed with water (5x10 ml). The organic layer was washed with brine, dried, and evaporated to isolate compound 12 (1.664 g) as dark brown oil. Yield was 84.3%.

2-(3-hydroxyphenyl)acetamide (13)

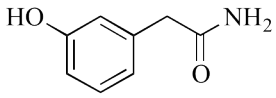

A schematic of the synthesis of 13 is shown in Figure 9. To compound 12 (1.0 g; 6.7 mmol) concentrated aqueous NH_4OH (6.5 ml) at 0℃ was added. The reaction mixture was stirred overnight at room temperature. The resulting solution was evaporated and the residue neutralized with AcOH. The solid obtained was recrystallized from hot n-butyl acetate (10 ml) to isolate compound 13 (0.57 g) as an off-white solid. Yield was 57.00%.

2-(3-Allyloxy-phenyl)-acetamide (14)

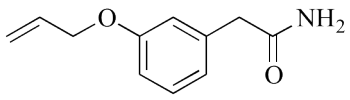

A schematic of the synthesis of 14 is shown in Figure 9. To a stirred suspension of compound 13 (0.5 g; 3.3 mmol) in dry acetone (10 ml) allyl bromide (0.48 g; 3.96 mmol) and potassium carbonate (0.49 g, 4.95 mmol) were added. The reaction mixture was heated at 70℃ overnight. The resulting solution was cooled to room temperature and filtered through a sintered funnel to remove solid residue. The filtrate was evaporated to dryness to isolate compound 14 (0.54 g) as a white solid. Yield was 100.0%.

2-{3-[3,-bis(nitrooxy)butoxy]phenyl}acetamide (15)

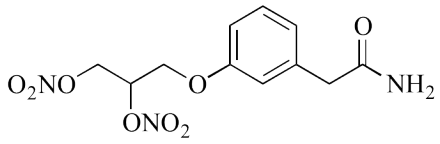

A schematic of the synthesis of 15 is shown in Figure 9. To an ice cooled, stirred solution of compound 14(0.5 g; 2.61 mmol) in acetonitrile (10 ml) silver nitrate (1.773 g; 10.44 mmol) was added. The reaction mixture was cooled in ice bath with stirring and iodine (0.664 g; 2.61 mmol) was added. After the iodine had dissolved, the reaction mixture became yellowish and was refluxed at 90℃ at room temperature for 12 hrs, filtered, poured into water and extracted with ethyl acetate. The organic layer was washed with brine, dried, and evaporated. The oil thus obtained was purified by flash chromatography (eluent from hexanes/EtOAc 10/1 to 3/1 v/v) to isolate compound 15 (0.615 g) as yellow oil. Yield was 71.6%. NMR results yielded: ^{1}H NMR ($CDCl_3$): δ 3.62 (d, 2H, J=2.4Hz), 4.28 (d, 2H, J = 4.92Hz), 4.80 (dd, 1H, J = 6.45Hz, J = 12.9Hz), 4.94 (dd, 1H, J = 3.51Hz, J = 12.9Hz), 5.39-5.40 (m, 2H), 5.61-5.64 (m, 1H), 6.84-6.86 (m, 2H), 6.96 (d, 1H, J = 7.77Hz), 7.30 (td, 1H, J = 2.04Hz, J = 6.08Hz); ^{13}C NMR ($CDCl_3$): δ 43.1 (CH_2), 64.7 (CH_2), 68.7 (CH_2), 76.6~77.4 (CH), 113.4 (CH), 115.6 (CH), 123.1 (C), 130.3 (CH), 136.6 (CH), 157.9 (CO), 172.7 (CON).

1.5 Nuclear Magnetic Resonance (NMR) Spectroscopy

^{1}H and ^{13}C-NMR spectra were recorded in chloroform-d on a Bruker Avance 300FT and 500FT instrument, respectively, using tetramethylsilane as internal standard. Spinwork was used to interpret the NMR spectra. Tetramethylsilane (0 ppm), residual chloroform in the chloroform-d (^{1}HNMR: 7.26ppm, ^{13}CNMR: 77.23ppm) and residual dimethyl sulfoxide in dimethyl sulfoxide-d6 (^{1}HNMR: 2.50ppm, ^{13}CNMR: 39.51ppm) were used as the chemical shift standard for ^{1}H spectra.

2. In Vitro Muscle-Fiber Culture Study

2.1 Animals

The Zebrafish used for this experiment were maintained and reared at 27℃ according to protocol number F12-034 of the University of Manitoba. This study was approved by the University of Manitoba Animal Care Committee and was in conformity with the Canadian Council on Animal Care guidelines. The length of selected Animal Care Facility zebrafish were between 30 and 40 mm and their weights were approximately 0.3g. Following dissection, fibers from two zebrafish were pooled for the experiment.

2.2 Tissue Dissection

All instruments were autoclaved before use and rinsed in 70% ethanol in advance to maintain sterility at all times. The anesthetic was prepared as the first step of dissection. Tricaine methanesulfonate (MS-222) (obtained from Animal Holding Facility, stored at 4 °C) was weighed (80 mg) and dissolved in 125 ml-warmed water. The fish were anaesthetized by MS-222 solution and moved to a plastic plate. The general fiber isolation process was as depicted below. The head and the tail of the fish were fixed on the plate with needles. In order to provide a sterile environment, ethanol (70%) was sprayed onto the entire fish and any excess was blotted off. After all the preparatory work had been completed, an incision was made along the ventral three quarters of the body along the dorsal side and the internal contents were removed. The skin and scales of fish were removed by forceps and the white adipose tissue on the dorsal side was gently and carefully removed to avoid damaging the muscle tissue. Finally, fine spring scissors were placed behind the gills to remove the head and the tail and fins were also removed and discarded. The remainder of the fish body was incubated in 15 ml tube with 2 ml Dulbecco's Modified Eagle's medium (DMEM) with 0.2% collagenase (see appendix 1) at 37℃.

2.3 Muscle fiber isolation

After two hours the contents were transferred to a 60 mm glass dish containing fresh L-15 proliferation medium (PM) (see appendix 1), which was prepared in advance and stored at 4℃. The dish contents were triturated by using the clean-cut end of wide pore pipette avoiding the production of any bubbles during the whole process. After the fish fibers were separated from the body, visible debris, including remaining bones, scales and fat droplets were removed manually using autoclaved forceps. In order to obtain sufficient fibers, the entire process was repeated. The medium with fish fibers was carefully transferred to a tube and the fibers allowed to settle after which, excess PM was then removed. The procedure was repeated using other fish and all the fibers were combined into one glass tube.

2.4 Plating fish muscle fibers

The entire process of plating was performed inside a biosafety cabinet (BSC) and all coverslips were cleaned and autoclaved prior to use. Before plating the fibers, collagen （Advanced BioMatrix, Inc., San Diego, CA）and the culture dishes were maintained on ice. The collagen was removed from the fridge and put onto ice along with plastic container holding the labeled dishes. Collagen (50 μL) was pipetted on the center of each coverslip and spread out

over the entire surface of coverslip with the clean-cut end of a wide bore pipette tip. Then, 30 μL of medium with fibers in it was transferred to the coated coverslip using the same type of wide bore pipette tip. The medium was also spread out evenly onto the surface of the collagen. Attention was paid to ensure that all the surfaces of the culture plates were in contact with the ice and maintained flat to allow all the fluid and fibers to be at same level at all times. This allowed the fibers to spread evenly in each dish. After covering the coverslips with fiber, lids were put onto the dishes and they were carefully transferred to a 27℃ incubator for 50 min. By doing so, the collagen was able to form a gel to which the fibers were attached.

Culture media was prepared in advance by adding the appropriate amount of BrdU to the total amount of L-15 basal growth media (see appendix 1) to have a 200 ngBrdU/ml stock. Seven different treatments were prepared for the experiment. The initial dose of MyoNovin and three of its analogs treatments were 1 mM. The positive control treatment group with ISDN were treated with an equimolar amount to provide the same amount of NO as the treatment samples. Since DMSO may cause damage to the muscle fibers and was added as the solvent for MyoNovin and its analogs, a treatment with DMSO was prepared as a negative control. Treatment with just BGM and BrdU also served as a control group.

Once collagen formed a gel, the dishes were transferred from the incubator to the biological

safety cabinet. Five hundred micolitres of treatment solution was added onto the coverslip and three replicates were prepared for each. After preparation the fibers were placed in a 27℃ incubator for 24 hours.

2.5 Fixing fish muscle fibers

The culture medium was discarded after 24 hours incubation and each coverslip was rinsed using 2 ml of sterile 0.01M PBS (see appendix 1). The fibers were fixed with 2 ml of prepared 5% acid alcohol (see appendix 1), which was made by diluting glacial acetic acid with ethanol. The fibers were allowed to fix for 20 min and were then dried for 45 min in the BSC. At this point, the fibers on the coverslips could be stored waiting for immunohistochemistry by adding 2 ml of 0.01M Tris-buffered saline (TBS) (see appendix 1), which contains 1% horse serum. Since in this study the fibers were used immediately, this storage procedure will not be described in detail.

2.6 Immunohistochemistry for BrdU

BrdU was used as a marker and it is incorporated into the satellite cells when they are in their S-phase. This process was assayed using anti-BrdU antibodies and to do this, several

procedures needed to be completed. First, each coverslip was washed twice (10 min each) with 2 ml 0.01 M PBS (diluted from 0.1 M PBS with distilled water). After washing, each dish was treated with 2 ml of 2 N HCl and was incubated at 37 °C for one hour. Washes needed to be done twice again also for 10 minutes per wash, this time using 0.01 M TBS-Tween 20 (TBS-T) (diluted from 0.1 M TBS with 1% Tween 20). Second, fibers were incubated for 1 hour at room temperature in blocking solution. The blocking solution used was goat serum (Invitrogen Corporation, Carlsbad, USA), which contained one of goat anti-mouse biotin-unconjugated antibody (Jackson Immuno Research Laboratories, Inc., West Grove, USA) for staining BrdU (diluted at the ratio of 20:1). One hour later, the coverslips were rinsed with 0.01 M TBS-T and were placed on parafilm. Tissue paper was placed underneath to maintain a humid environment and the foil layer was incubated with 0.001% avidin and 0.001% biotin for 15 minutes respectively. After these two blocking steps, fibers in anti-BrdU antibody were incubated overnight in primary antibody (anti-BrdU antibody (Roche Applied Science, Penzberg, Germany) (see appendix 1).

On the second day of Immunohistochemistry, the fibers were first washed twice with 0.01 M TBS-T and then incubated with 3% H_2O_2 for 10 minutes. After incubating, the fibers were washed again twice (10 min each) in 0.01 M TBS-T. Biotin-conjugated anti-mouse IgG (Jackson Immuno Research Laboratories, Inc., West Grove, USA) (see appendix 1) worked as the

secondary antibody for staining BrdU. The fibers were incubated at room temperature for another hour, and then washed twice with 0.01 M TBS-T. This process of incubating and washing was repeated but this time, incubation was with a 1:500 solution of streptavidin conjugated with horseradish peroxidasein (HRP, Vector Laboratories Inc., Burlington, CA, USA) in 0.01 M PBS at RT for 20 minutes. Finally, fibers were incubated for the last time in a diaminobenzidine (DAB, Sigma Aldrich, St. Louis, MO, USA) working solution, which included 0.01 M PBS, DAB, color intensifier and 3% H_2O_2. This solution generates a dark brown stain over nuclei by reacting with HRP after incubation at room temperature. After 5-7 minutes the reaction was stopped by washing the coverslips with water.

2.7 Analysis and Statistics for Muscle-Fiber Culture Study

Coverslips with different treatments were viewed using an Olympus BH2 light microscope to count BrdU+ stained cells. Cells were scanned across each dish for intact fibers under the microscope without knowledge as to which group the coverslip belonged. As the average number of fibers per dish was 25, at least 80 fibers were observed in each treatment group. A 400X magnification was used to examine each fiber and the satellite cells with dark brown nuclear staining were counted.

To evaluate the level of SC activation, defined by incorporation of BrdU during the S-phase of the cell cycle, the number of SC per fiber that stained positive for BrdU was counted. At least 20 fibers per dish were observed by scanning across the coverslip or dish and counts were only recorded for the intact fibers that were separated from one another, again without knowing the treatment group the sample belonged too. When evaluating the level of SC activation with BrdU positive staining only the nuclei that were stained dark brown were counted as positively stained.

After counting the number of BrdU-positive SC per fiber, data were presented as mean±SEM and analyzed using Microsoft Excel. The number of BrdU+ nuclei (activated SCs) was plotted on the y-axis against the different treatment groups on the x-axis. The significance of the changes in SC activation with the different treatments was carried out using two-sample t test with equal variance followed by a one-way ANOVA for multiple comparisons.

3. Water Solubility studies

3.1 Sample preparation

Each vial was labeled according to treatment with capital letters and experiment code (from 1-5). For the MyoNovin group, vials were labeled as vial A1 to A5. MyoNovin was weighed out

at 0.15 mmol（4.32 mg） and added to vial A1. Acetone (0.75 mL) was added to this vial and after mixing, A 0.1mL volume of the solution was transferred to the next vial – vial A2. Extra acetone (0.9 mL) was added this time to make a 2 mM MyoNovin/acetone solution. From this 2 mM solution, 0.1 mL was transferred to the vial A3 and this was followed by adding 0.9 mL of acetone. This process was repeated until the vial A5 contained 1mL of 0.002 mM MyoNovin/acetone solution. The same procedure was applied to the other three analogs. By doing so, a 10-fold dilution was prepared in order to provide samples within a reasonable detection range. Within each group, five stock solutions with different concentrations (0.002 mM, 0.02 mM, 0.2 mM, 2 mM and 20 mM) resulted and correspondingly left with 1, 0.9, 0.9, 0.9 and 0.65 mL of solution. Each stock solution (100 μL) was seeded into the well of a 96-well black plate and each concentration was repeated in triplicate (see Table 2 for the plate layout). The plate was left to air dry stored in a biosafety cabinet overnight.

The next day, a Synergy™ HT Multi-Detection Microplate Reader was used and absorbance measurements at 630 nm were recorded using the Gen5 software. After 1 hour, absorbance was read and recorded again and the result was compared with data from first test. This confirmed that all the solvent (acetone) in the wells were evaporated as two test result were similar. These wells were then filled with 200 μl of double-distilled water. In addition, four blank wells also received 200 μl of double-distilled water as negative control. The plate was

shaken for 24 hours until equilibrium was reached. After shaking, the plate was inserted into the reader again and the absorbance at 630 nm recorded. After 30 minutes, absorbance was read and compared to the date abstained last time to make sure equilibrium had been reached. The results were recorded and exported directly to Excel©.

Table 2 Plate layout for solubility study

	1	2	3	4	5	6	7	8	9	10	11	12
A	10mM MN1	1mM MN1	0.1mM MN1	0.01mM MN1	0.001mM MN1	10mM MN2	1mM MN2	0.1mM MN2	0.01mM MN2	0.001mM MN2	10mM MN3	1mM MN3
B	10mM MN1	1mM MN1	0.1mM MN1	0.01mM MN1	0.001mM MN1	10mM MN2	1mM MN2	0.1mM MN2	0.01mM MN2	0.001mM MN2	10mM MN3	1mM MN3
C	10mM MN1	1mM MN1	0.1mM MN1	0.01mM MN1	0.001mM MN1	10mM MN2	1mM MN2	0.1mM MN2	0.01mM MN2	0.001mM MN2	10mM MN3	1mM MN3
D	10mM MN1	1mM MN1	0.1mM MN1	0.01mM MN1	0.001mM MN1	10mM MN2	1mM MN2	0.1mM MN2	0.01mM MN2	0.001mM MN2	10mM MN3	1mM MN3
E	0.1mM MN3	0.01mM MN3	0.001mM MN3	10mM MN4	1mM MN4	0.1mM MN4	0.01mM MN4	0.001mM MN4	Water			
F	0.1mM MN3	0.01mM MN3	0.001mM MN3	10mM MN4	1mM MN4	0.1mM MN4	0.01mM MN4	0.001mM MN4	Water			
G	0.1mM MN3	0.01mM MN3	0.001mM MN3	10mM MN4	1mM MN4	0.1mM MN4	0.01mM MN4	0.001mM MN4	Water			
H	0.1mM MN3	0.01mM MN3	0.001mM MN3	10mM MN4	1mM MN4	0.1mM MN4	0.01mM MN4	0.001mM MN4	Water			

MN1 represents MyoNovin and MN2, MN3 and MN4 refer to three MyoNovin analogs. They were all assayed at five different concentrations. Note water was also run for the test as a control.

IV. Result

1. ^{1}H and ^{13}C NMR Spectra

^{1}H NMR and ^{13}C NMR of MN1-4 are illustrated from Figure 10 to Figure 17.

Figure 10 MN1 1H NMR Spectra

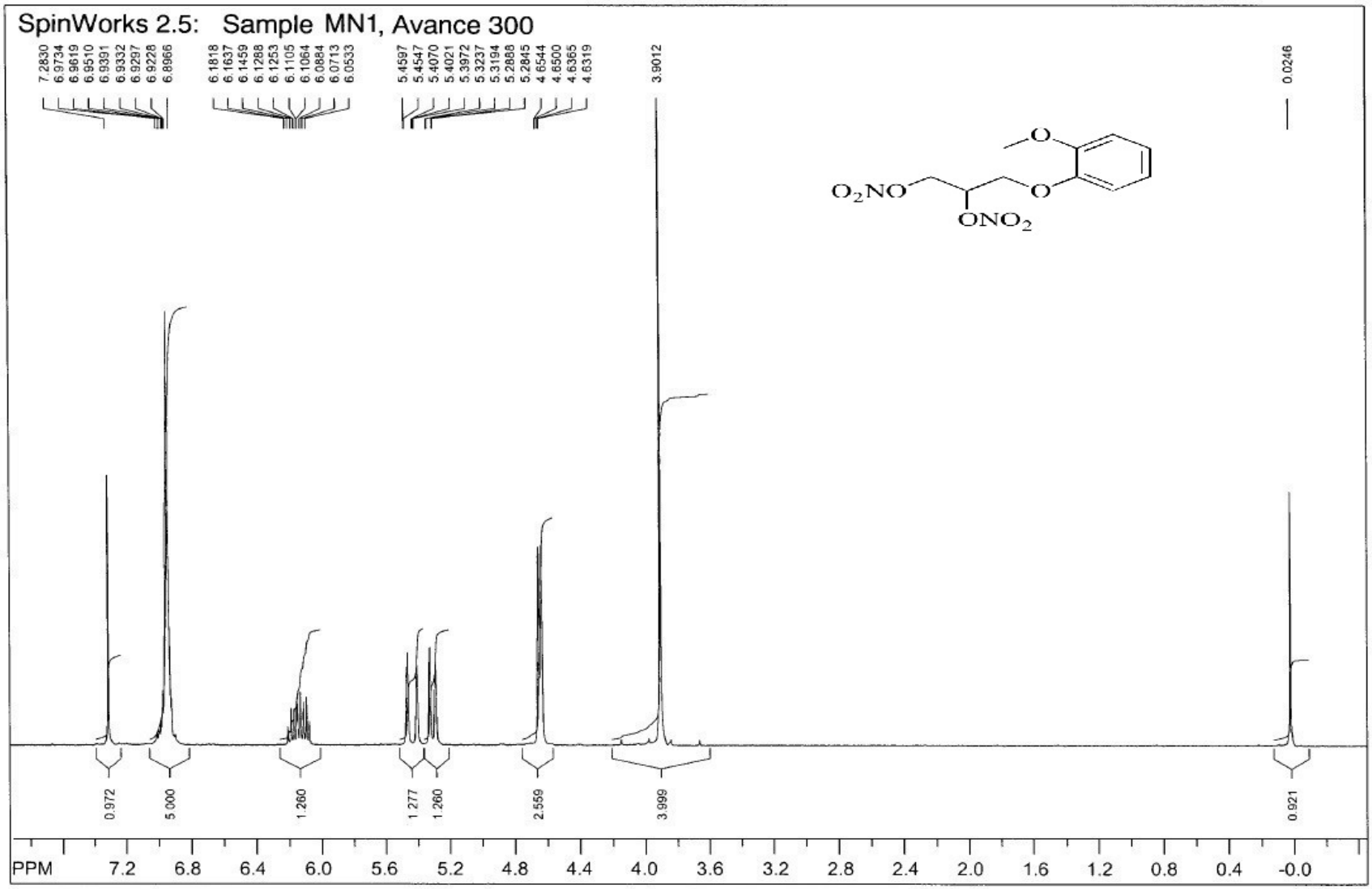

Figure 11 MN1 13C NMR Spectra

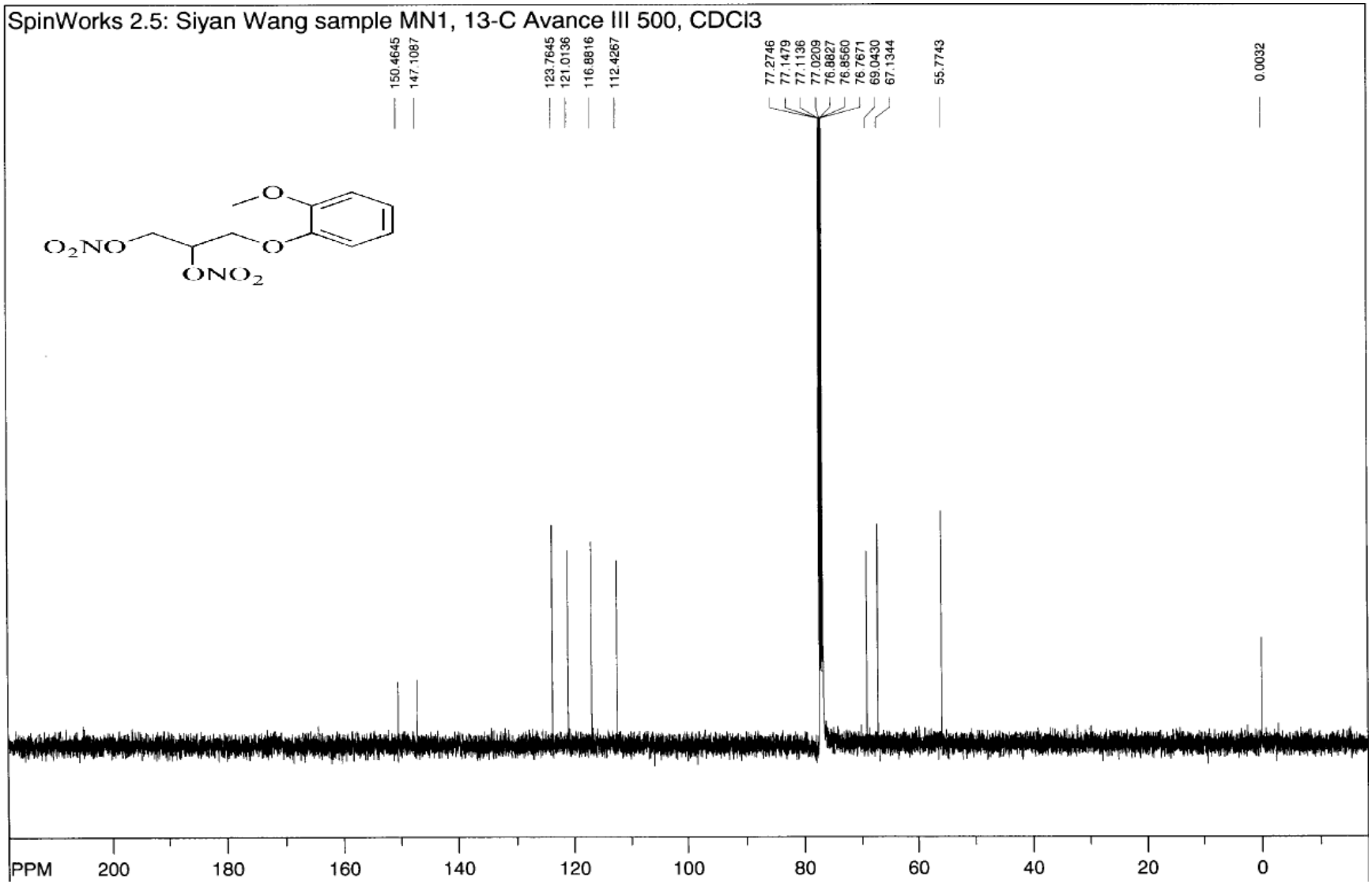

Figure 12 MN2 1H NMR Spectra

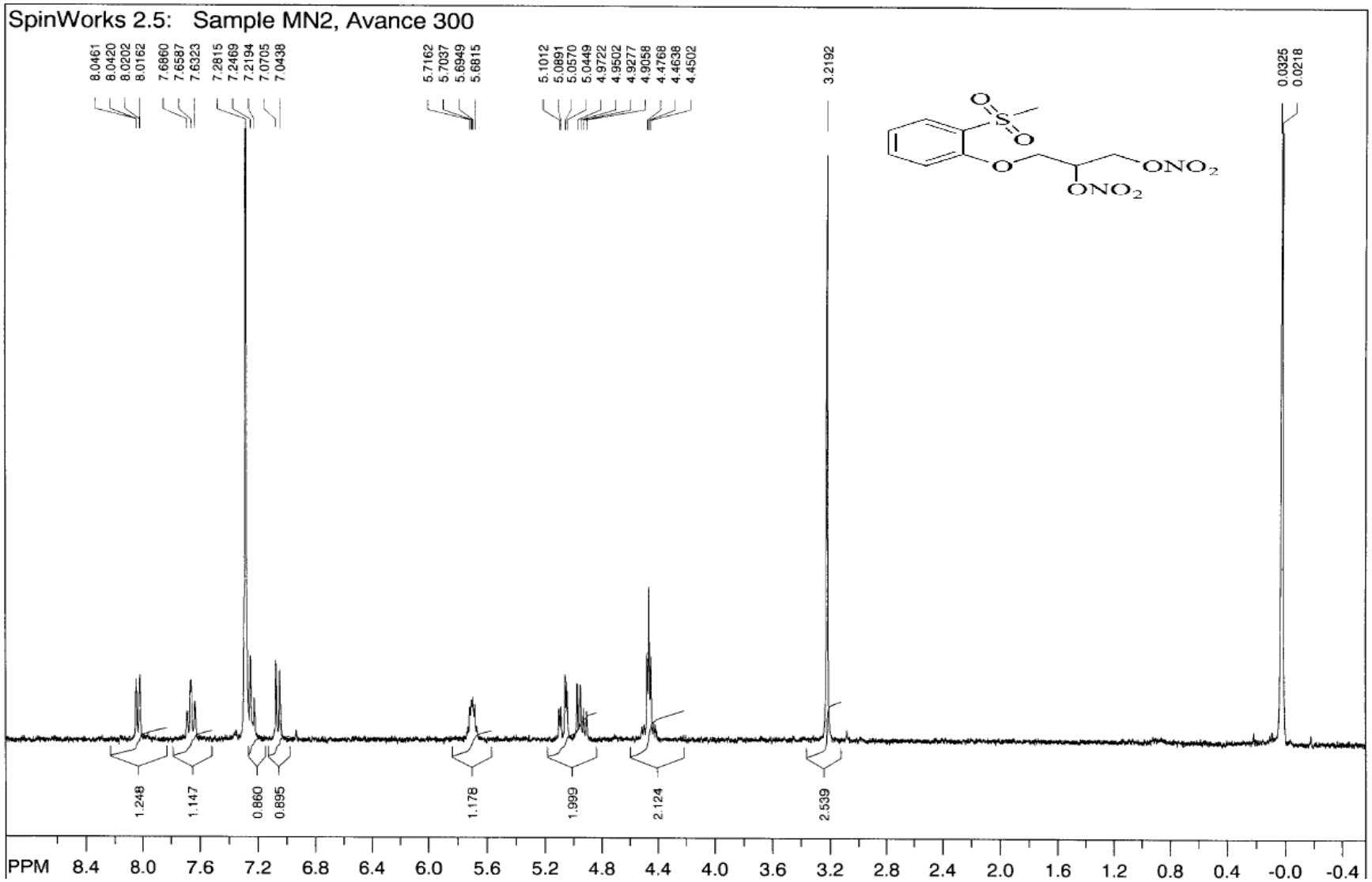

Figure 13 MN2 13C NMR Spectra

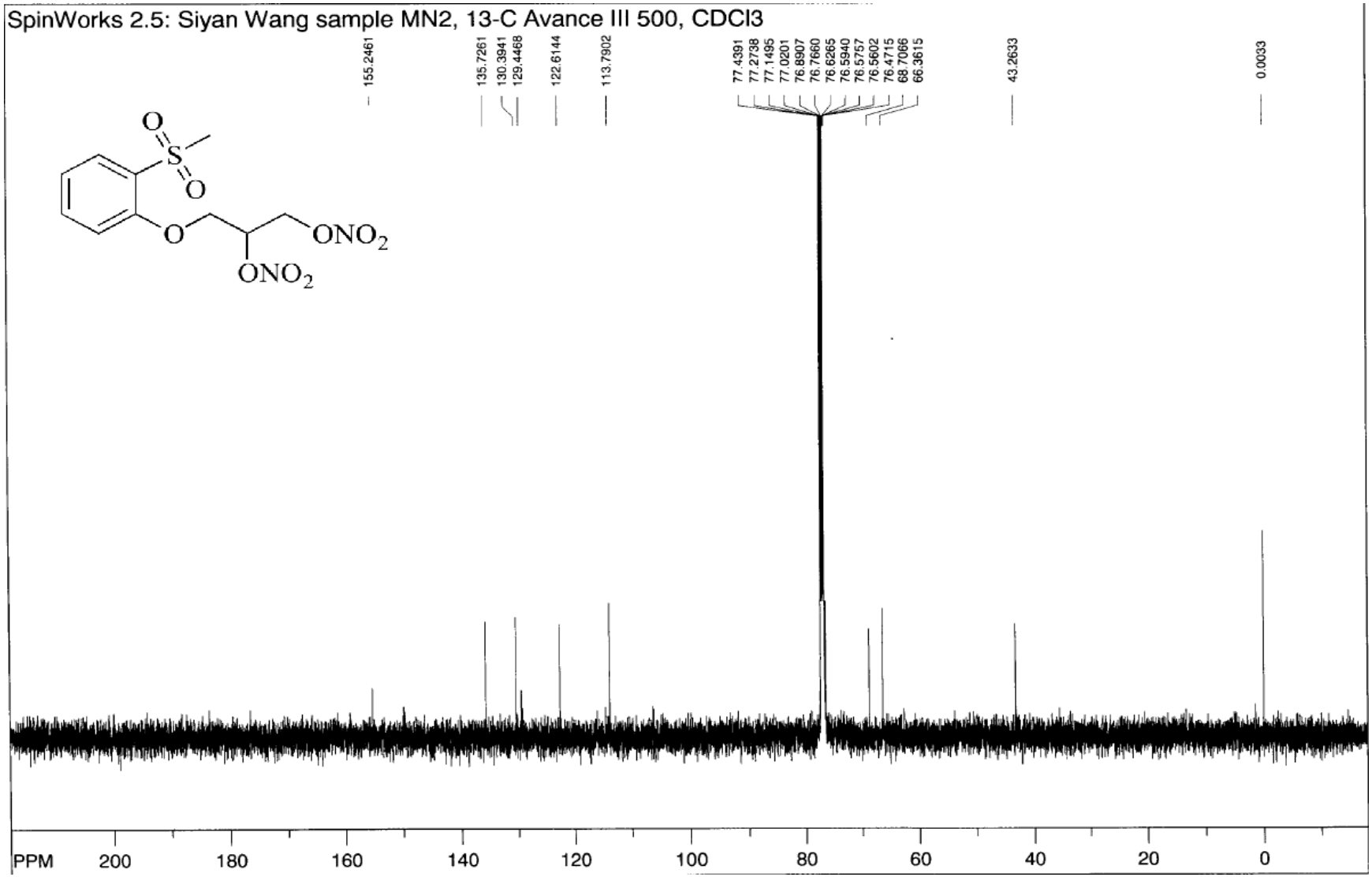

Figure 14 MN3 1H NMR Spectra

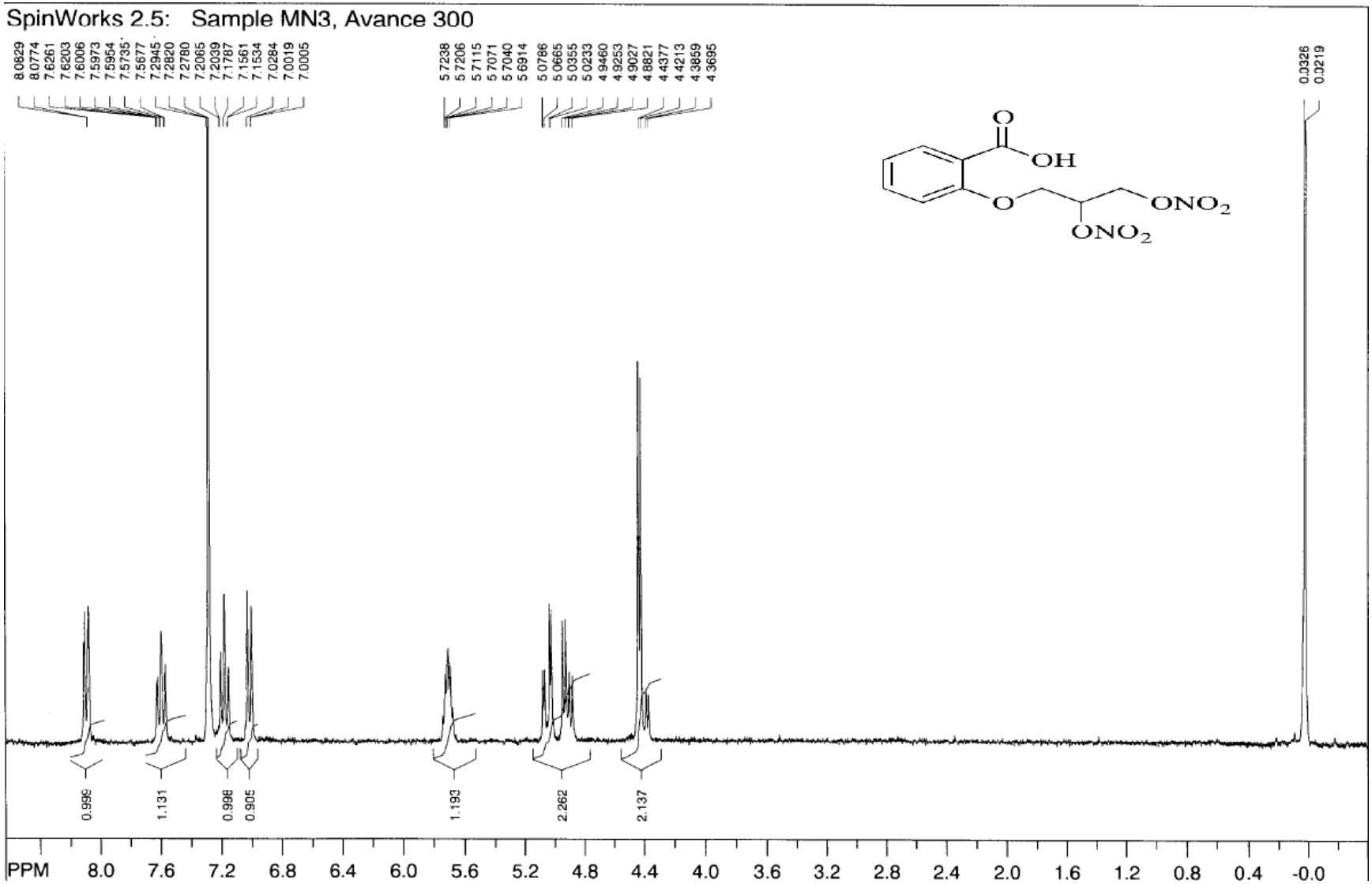

Figure 15 MN3 13C NMR Spectra

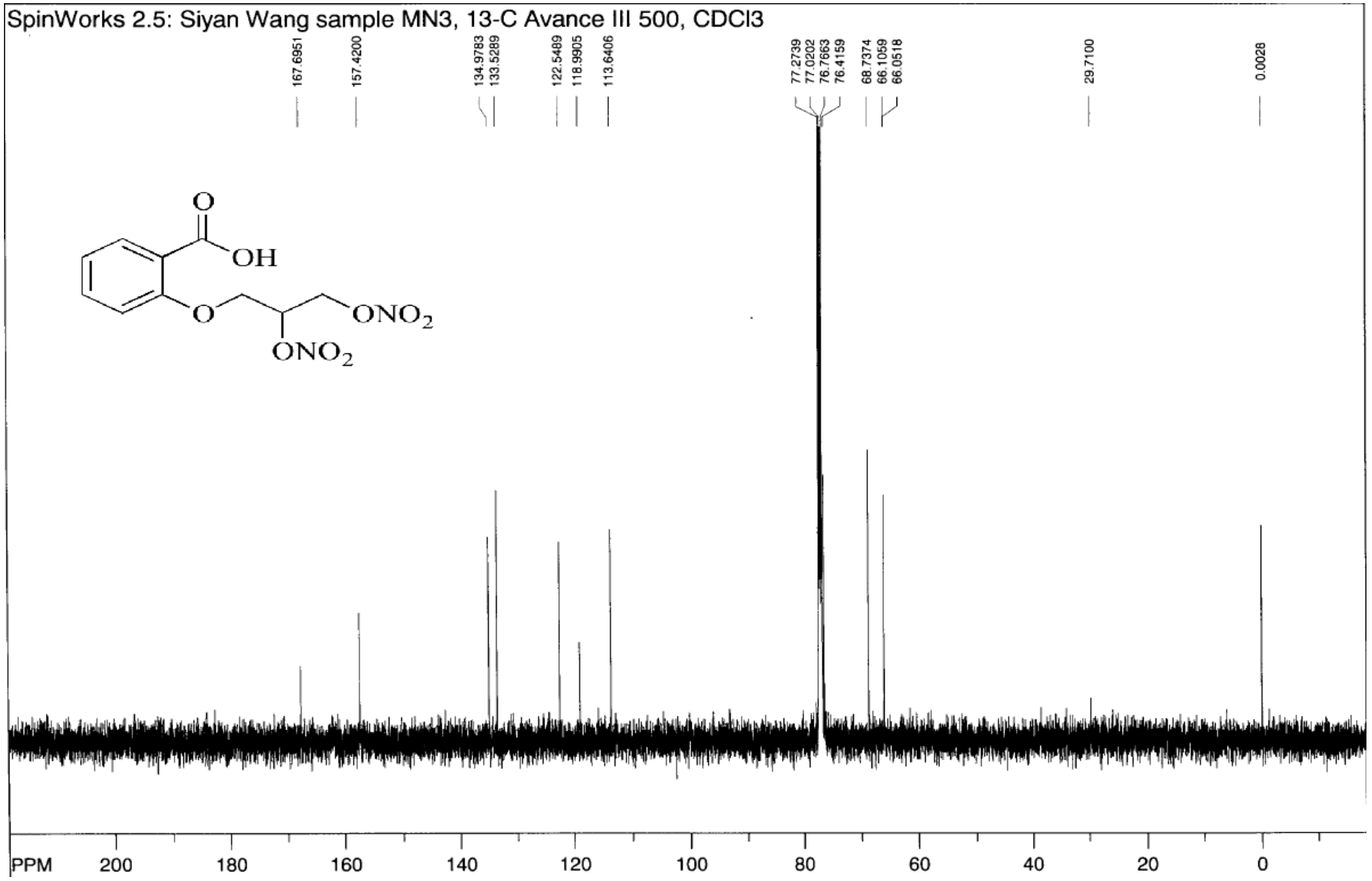

Figure 16 MN4 1H NMR Spectra

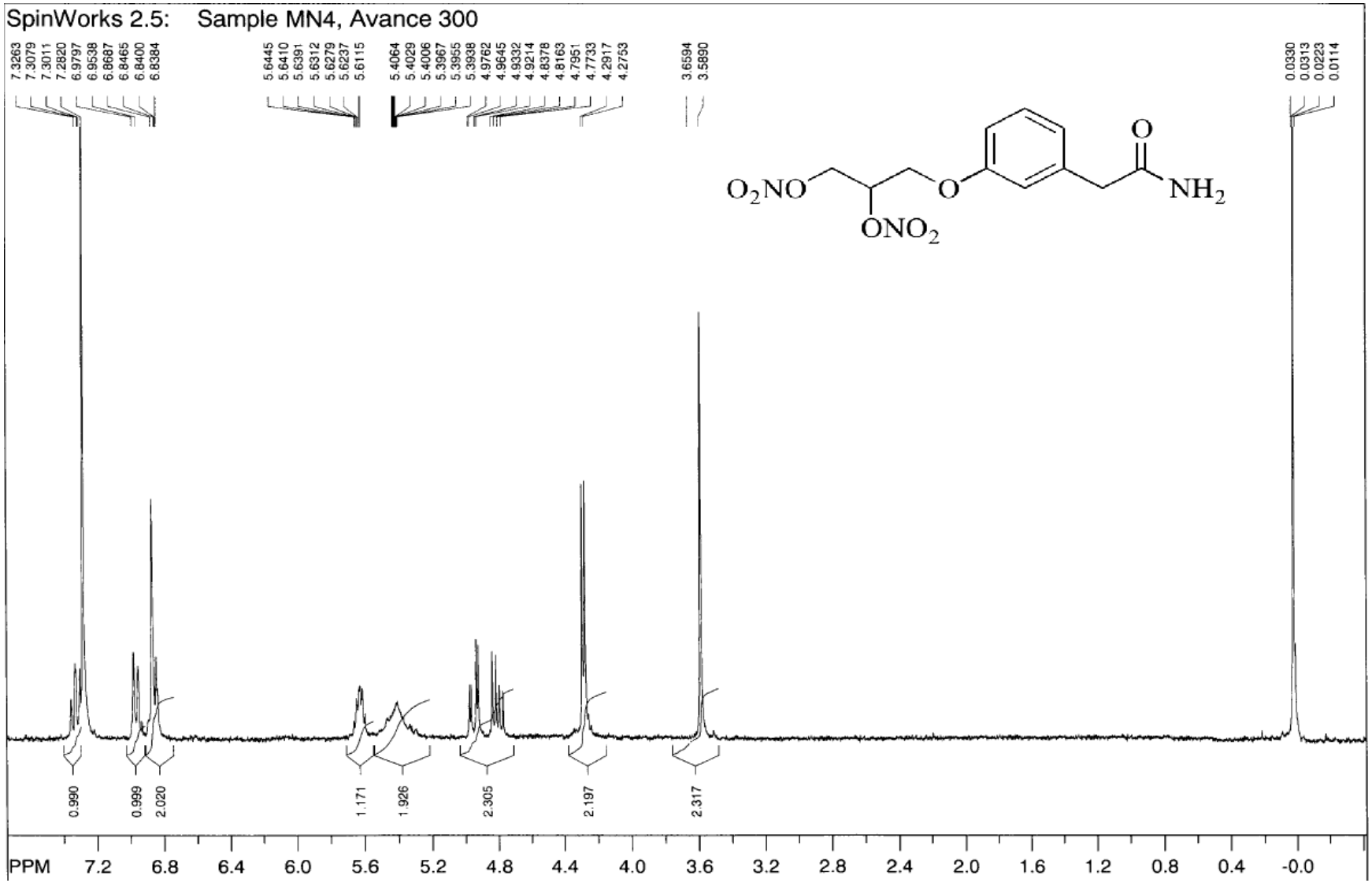

Figure 17 MN4 13C NMR Spectra

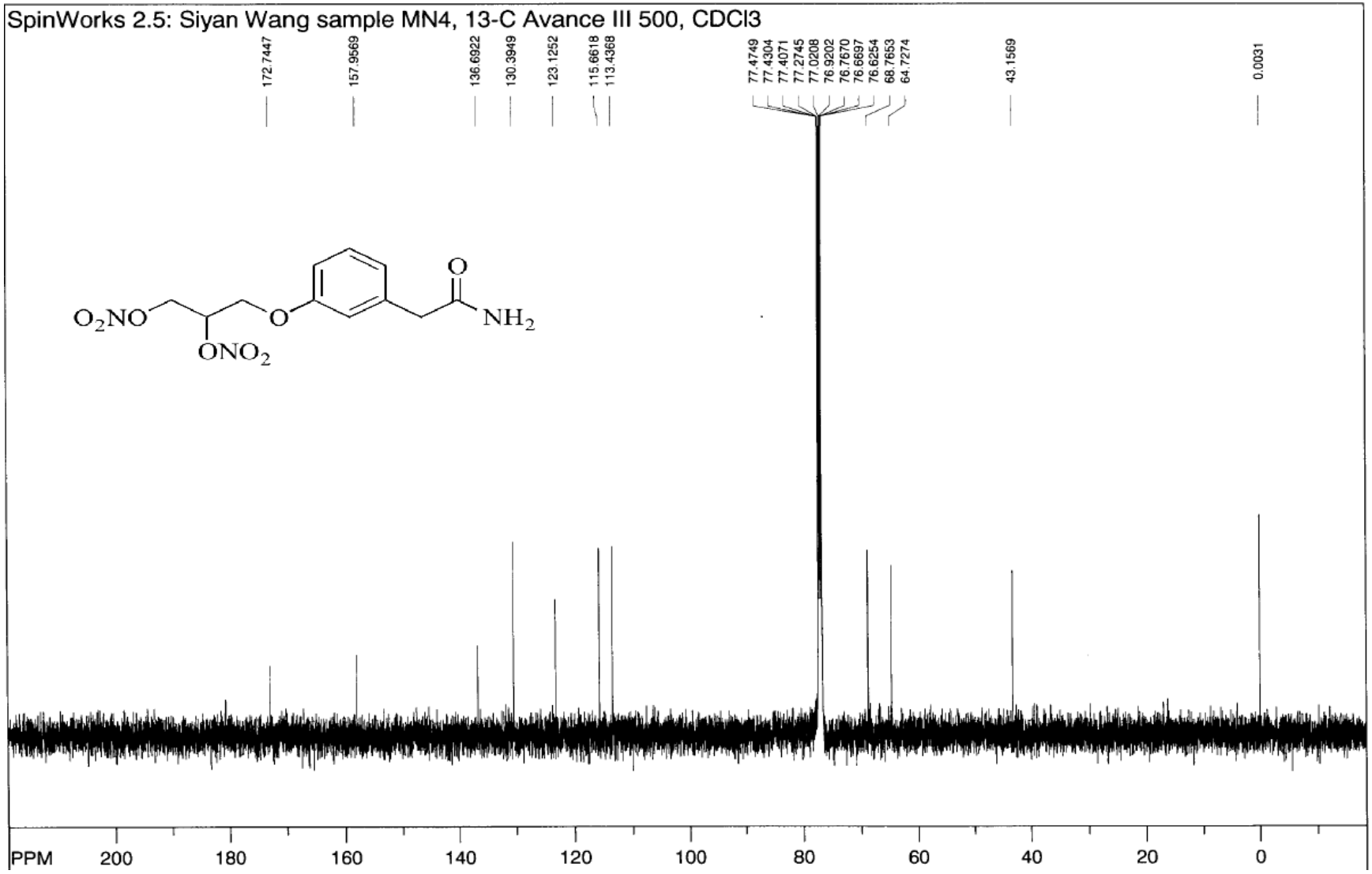

2. In Vitro Muscle-Fiber Culture Study

The activation of satellite cells (SC) can be tested by detecting DNA synthesis, measured by BrdU incorporation into cells that are activated and specifically enter the S-phase of cell cycle. As shown in Figure 18, satellite cell activation was demonstrated by plotting the number of BrdU positive satellite cells per fiber (mean ± SEM) vs treatment group. The number of BrdU positive SCs per fiber in the different MyoNovin-analog treatments showed the activation levels for the MyoNovins when compared with positive treatment (ISDN, 1mM) and negative control (DMSO, 1mM and BGM). The number of BrdU+ SCs per fiber of the three analogs (MN2, MN3 and MN4) was 3.30 ± 0.007, 3.32 ± 0.005 and 3.14 ± 0.016, respectively, which was significantly different from the DMSO control group (2.66± 0.013). This result suggests that the level of satellite cell activation showed a significant response to the three MyoNovin analogs. When compared to the positive treatment with ISDN, the three MyoNovin analogues showed a significant difference to ISDN ($p<0.001$; ANOVA), which means at least one analog either did not display strong ability of activating satellite cells or showed extra strong ability. By testing with two-sample t-test with equal variance, the result shows that MN2 and MN3 did not have a significant difference with ISDN treatment while MN4 was just the opposite with 95% confidence (a significance level of 0.05). This result suggests that MN4 did not display strong

ability when activating satellite cells. As MyoNovin (MN1) was shown to have the ability of activating satellite cells, it was considered as a positive control for this analysis. From the two-sample t-test, none of three MyoNovin analogs displayed a significant difference when compared to MyoNovin. Thus, they shared similar activity in activating satellite cells. When compared with the negative control (DMSO), all three analogs resulted in a significant increase in DNA synthesis with 95% confidence (a significance level of 0.05). This result, taken in aggregate with the other two statistical analyses above, suggests that all three MyoNovin analogs have different degrees of bioactivity. As MN2 and MN3 displayed no significant difference when compared to MyoNovin or ISDN, their ability to increase DNA synthesis are better than MN4, which did not display any better activating potential when compared to ISDN.

2. Water Solubility Studies

The purpose of these studies was to understand the solubility differences in MyoNovin and the synthesized analogues. To test the hypothesis that the MyoNovin analogs have better water solubility than MyoNovin, the light transmittance in the presence of each compound at five different concentrations was determined as shown in Figure 19. Statistical analysis was applied for each target compound to test the significance between 10 mM with the other four

concentrations. As seen from figure 19, MyoNovin (MN1) showed a decreased absorption from 1 mM to 0.01 mM and then leveled off which indicated that the solubility of MyoNovin in water is between 0.01 mM to 0.1 mM. The curves for MN2 and MN4 stopped decreasing and become stable at 0.1 mM, which suggested that the true solubility value should be obtained in the range from 0.1 mM to 1 mM. Likewise, the water solubility value for MN3 is between 1 mM to 10 mM. Thus, the water solubility of MyoNovin is likely between 0.01 mM to 0.1 mM，while the water solubility of the novel MyoNovin analogs are likely between 0.1 mM to 10 mM with MN3 showing the best water solubility.

Figure 18 Satellite Cell Activation

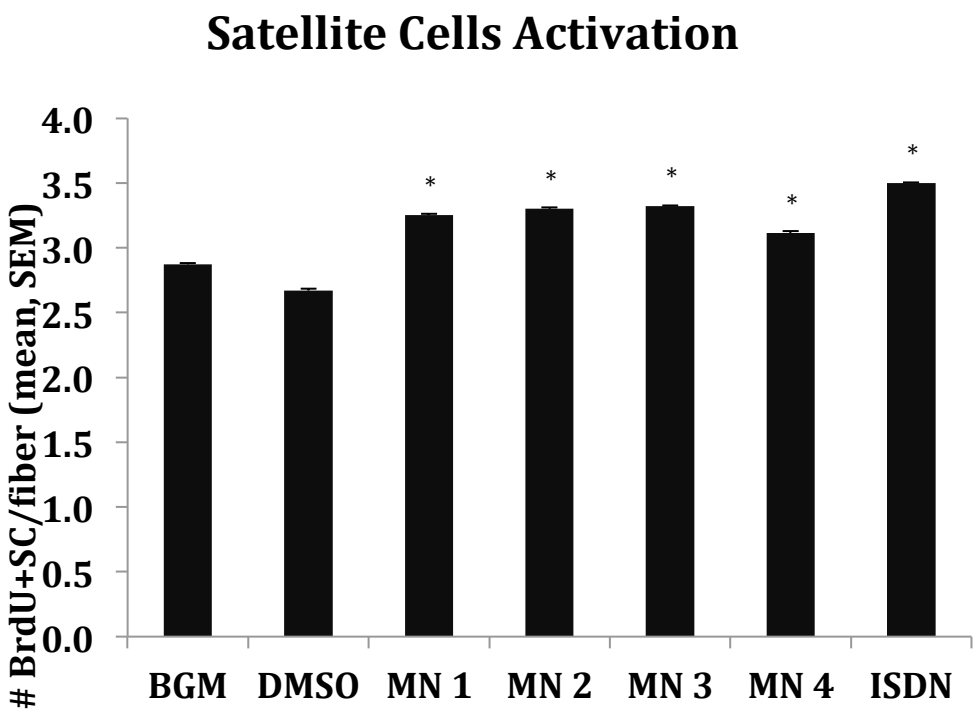

Bar graphs showing the satellite cell activation studies resulting from different treatments with MyoNovin (MN1), MyoNovin analog 1(MN2), MyoNovin analog 2(MN3) MyoNovin analog 3(MN4), positive treatment with ISDN and two negative control groups (BGM and DMSO). Concentrations of all treatments except BGM were 1 mM. All three MyoNovin analog groups had statistically activated satellite cells in fish fibres. Band densities were quantified and expressed as mean ∆ SEM., n=79-94, * $p < 0.05$ compared to control group.

Figure 19 Water Solubility Study

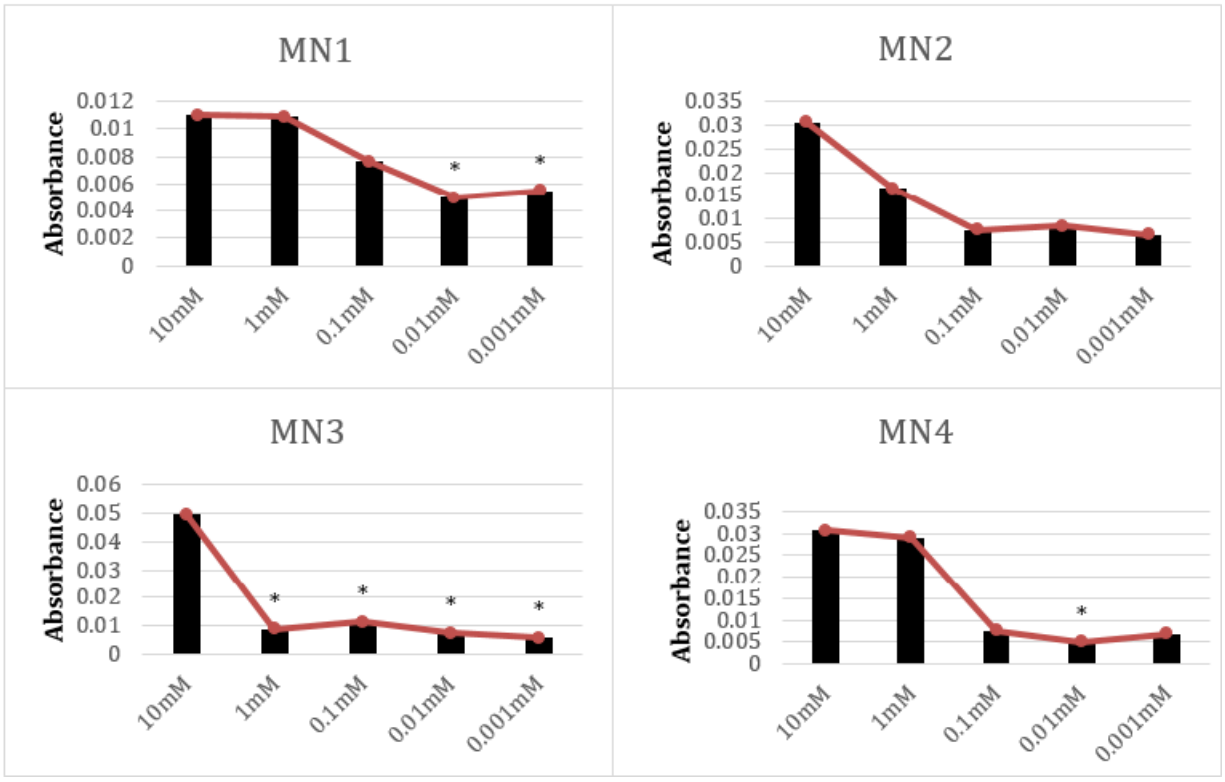

* $p < 0.05$ compared to 10mM treatment group

Bar and line graphs showing the water solubility studies resulting from different concentrations of MyoNovin (MN1), and MyoNovin analog 1 (MN2), MyoNovin analog 2 (MN3) MyoNovin analog 3 (MN4). The graph of MyoNovin (MN1) showing a decreased absorption from 1 mM to 0.01 mM, which indicated that, the true value of MyoNovin water solubility is between 0.01 mM to 0.1 mM. Compared to MyoNovin, water solubility of the three analogs are increased to varying degrees. * $p < 0.05$ compared to 10 mM treatment group.

V. Discussion

Given the explosion of medical research there are still significant difficulties in developing new drugs. For a desired drug, safety and efficacy are paramount. Besides ADME (absorption, distribution, metabolism and excretion), stability and water solubility are other factors that need close attention. These are especially important in formulation development. The purpose of this investigation was to chemically modify a compound that has very good biological activity but very poor properties for formulation development. MyoNovin was selected as a lead substance by its proven pharmacological activity in activating satellite cells and promoting muscle regeneration. MyoNovin, however, has very limited water solubility. Modifying the structure of MyoNovin with functional groups that have higher water-solubility characteristics should enhance the overall water solubility of the molecule and make formulation development easier. By doing this, novel MyoNovin analogs were developed and their biological function tested. The work on designing the potential structures and solubility are discussed below.

1. Potential structure design

1.1 Pharmacophore and functional group modification

For a drug molecule, only part of the structure is normally responsible for its biological activity. Pharmacophore is the word we use to describe the relevant groups that provide pharmacological activity. The approach to modify the lead compound is to keep the main pharmacophore intact and replace other more superfluous functional groups. In this investigation, the aim was to deliver nitric oxide to the muscle fiber. Based on the structure, two nitrate groups linked by a chain with appropriate length have the ability to release two molecules of nitric oxide *in vivo*. In organic chemistry, nitrates are represented by the grouping $RONO_2$ where R stands for any organic residue. Organic nitrates, which can be classified as prodrugs, can generate nitric oxide by undergoing a denitration. From the discussion above, the pharmacophore is safely identified and modification of the structure may proceed. Methoxy and phenyl groups are considered as two superfluous functional groups that can be replaced. In the present design, the methoxy group was modified by methanesulfonyl (MN2), acetic acid (MN3) and acetamide (MN4). Based on Hajduk's study [86], the **ΔClogP value of** these three functional groups were -1.6, -0.3 and -1.7, respectively, which are different from the methoxy group (-0.1). ClogP value of a compound is used to calculate the logarithm of the equilibrium concentration of solute in

n-octanol divided by the concentration of the same species in water. Theoretically, high hydrophilicities are shown by low ClogP values. Therefore, the selected functional groups have, in theory, better solubility than the methoxy group. In the solubility study, results show that the solubility of all three compounds increased by almost one order of magnitude, which provides support for the hypothesis that the new MyoNovin analogues will have increased the water-solubility by modifying the structure with functional groups that have the high potential for water solubility.

1.2 Water solubility

Structure modification mainly changes the water solubility of MyoNovin. The software Marvin Sketch developed by ChemAxon was used in our investigation to predict a compound's water solubility based on its structure topology. Predicted water solubilities of MN1, MN2, MN3, and MN4 were 0.1 mM, 0.35 mM, 0.16 mM and 0.44 mM, respectively. These predictions disclosed that water solubility of the three MyoNovin analogs increased by various extents after changing their structure. These results also strongly support the current experimental results. Current result shows that the solubility of MyoNovin in water is between 0.01 mM to 0.1 mM which is consistent with the predicted result. Experiment results for MN2 and MN4 suggested

that the true solubility value should fall in the range from 0.1 mM to 1 mM, while the water solubility value for MN3 is between 1 mM to 10 mM. The value of predicted water solubility of MN2 and MN4 were inside the range that may contain the true value for the water solubility obtained by the water solubility study. In addition, as an organic acid, with the raising of pH the aqueous solubility of MN3 increased markedly. Therefore, as the water solubility of MN3 depends strongly on the pH of the solution, it may likely have different values, as the pH changes.

1.3 Other changed parameters

The main purpose of the different modifications was designed to enhance the solubility of MyoNovin, but during the modification process solubility may not be the only parameter that changes. Other drug-like properties such as pharmacological activity also could change when the structure changes.

Structure modification may influence the extent of biological activity. In these investigations, the *in vivo* fish muscle-fiber study was used to evaluate the influence of structure modification. The number of BrdU+ SCs per fiber of the three MyoNovin analogs (MN2, MN3 and MN4) was 3.30 ± 0.007, 3.32 ± 0.005 and 3.14 ± 0.016, respectively, while the result of

MoyoNovin was 3.25 ± 0.009. This result suggests that some of the structure modifications increased bioactivity but others act in the opposite direction. This kind of difference may actually be relevant to inductive effect. Inductive effect is an electronic effect due to the electronegativity difference between two atoms forming a sigma bond. Electrons are pulled by the more electronegative atom makes electron density shift to one direction. The reason why inductive effect becomes a potential explain is that for the MN2 and MN3, which increase the bioactivity, are considered as electron-withdrawing and conversely the only one (MN4 with acetamide group) that negative impacts the bioactivity was modified with a electron-releasing group. This hypothesis, however, needs to be tested. Quantitative structure - activity relationship (QSAR) could be an appropriate and effective analytical method for testing this hypothesis. Dimensional QSAR approach is useful in drug design studies to establish a structure-related physiological activity model by analyzing a molecule's physiological activity using the properties of the entire molecular structure as parameter. Common structural features include: hydrophobic features, electrostatic features, steric features, physical and chemical properties, geometric features and topological features. By analyzing these features, the QSAR approach will describe variations in which feature of the training set can lead to the increase or decrease of satellite cell activation. To increase accuracy, more compounds with different modifications need to be synthesized and their bioactivities evaluated. As MyoNovin releases nitric oxide possibly by non-enzymatic and

enzymatic pathways [102], 3D-QSAR could be used to have more explicit physical significance and much more information. 3D-QSAR can reflect the nonbonding interaction characteristics of the interactions between drug molecules and receptor. A number of enzymes (such as glutathione-S-transferase) have been shown to catalyze the production of nitric oxide that could be used as a receptor [103]. It is thus possible to increase the nitric oxide release by interacting with these enzymes.

2. Establishment of solubility measurement

The overall propose of this thesis project was to modify MyoNovin and examine the water solubility enhancement of three novel MyoNovin analogs. With the advancement of science and technology, a growing number of new operating processes and new measurement technologies have emerged. A good high efficiency solubility measurement must have the following characteristics: 1）a relatively short measurement time; 2）small error；3）have reproducible high-throughput procedures; and 4) minimal amounts of sample required.

The shake-flask approach is the most traditional equilibrium method and likely the best method to measure solubility if wide a range of different samples needs to be tested. Although the classical shake-flask method was standardized when designing aqueous solubility studies, it still

cannot meet the requirements of current solubility determinations. The major problems include test samples being consumed in large quantities, the possibility of automation is quite low, and the whole process is very time consuming. To overcome the former two disadvantages, 96-well or 384-well microtiter plate-based methods with dispersion techniques became viable replacements of the traditional shake-flask method. The improvement is to reduce the amount of the sample. As each well usually requires 100 μL~200 μL of solution, the amount of required compound is reduced. Several studies [87,104] showed that the reduced solvent volume to 0.05 mL per test does not affect the measurement accuracy of the method. The majority of experiments using the shake flask method test drug solubility [104,105] using solvent volumes within a range of 50 ml~300 ml. In the present studies, 96-well microtiter plate-based method was applied in order to reduce the amount of MyoNovin and introduce some level of automation to the procedure. The amount of compound required was reduced to approximately 5 mg for the entire testing process including three duplicates for each group. This becomes important when synthesis of the drug is costly or when poor yield may be expected.

When the main requirement is to measure solubility quickly then the kinetic method is arguably preferred. This method requires much smaller amounts of material and automation is possible. However, some drawbacks merit discussion before using this method. This method is not particularly precise as the organic solvent involved could influence the solubility.

Nevertheless, the time and volume advantage of this approach makes it a first choice for solubility measurements. It also becomes an optimal measurement method in the early stages of the drug discovery process mainly because of the lower amount of sample required and higher measurement speed, which makes it suitable for drug screening.

In the present study, similar principles based on both the equilibrium and kinetic methods were used. In the present study, we set the equilibrium time， prolonged to 24 hours, which was defined as a good way to get a more accurate solubility and acetone is removed by evaporation before measuring the solubility. In order to ensure that 24 hours is sufficient time to reach equilibrium, absorbance was tested twice at 30-minute intervals and compared to make sure equilibrium is reached. This method is convenient as it obtains the solubility data just in one step. Compared with the kinetic solubility method, the measuring efficiency of this method has been reduced mainly due to the increase of one preparation step of test material as well as the entire equilibrium time. In this method, the solvent acetone is removed by evaporation at the beginning of the experiment, so the effect of the solvent is also significantly reduced or totally eliminated. In addition, this method is similar to the equilibrium solubility measurement method, which also uses solid materials as the measurement test material, thus the risk of forming a saturated solution due to the co-solvent is reduced.

3. Satellite Cell Activation

In recent years, several compounds have been discovered for treating muscular dystrophy by combining two drugs. In this way, these novel compounds can have additional nitric oxide releasing activity other than their native properties. HCT 1026 is a combination of NO-releasing drug and non-steroidal anti-inflammatory drug (NSAID) and has significant and effective therapeutic effects in muscular dystrophy [106]. Another compound that has both NO donation property and cyclooxygenase inhibiting activity is NCX 320 [107]. These compounds, including MyoNovin, look promising for their advantages over a conventional single drug but, how these modifications would change the activation is unpredictable. One of the aims of this thesis was to examine the effect that changes structure modification has on satellite cell activation using a zebrafish muscle-fiber culture system. The results explained that MN2 and MN3 showed good satellite cell activation as we expected while MN4 is less effective in activating satellite cells on zebrafish fibers. This observation is contrary to what one would expect especially when comparing to solubility data. MN4, which have less bioactivity, is more soluble when compared to MyoNovin 1. This could be due to two factors. First, in an effort to analyze the activation of satellite cell in zebrafish fibers, DMSO was added to dissolve each target compound. This allowed compounds to be fully dissolved but offered hardly any clue as to the effect of the

solubility enhancement. Nonetheless, results suggested that three analogs had activated satellite cells and had operated on zebrafish muscle fibers. Another possible explanation for this phenomenon is that the structure modification may affect the bioactivity of novel MyoNovin analogs. For MyoNovin 4, the modification may have influence on the release of two nitro groups, which is an important step for NO donors to be effective.

4. Limitation and Future Direction

In the present water solubility study, these data provided supporting evidence for structure modification showing beneficial influence on enhancing the water solubility. However, one possible limitation of our study, which should be noted, was that we were unable to obtain the true value of water solubility of each compound. In an effort to make a precise conclusion about the water solubility, it would be better to perform a shake-flask method measured by HPLC.

VI. Conclusion

The research work discussed in this thesis can be summarized as follows:

(1) In the present study, three MyoNovin analogs have been developed for enhancing the water solubility of the lead compound – MyoNovin.

1-(2,3-Bis-nitrooxy-propoxy)-2-methanesulfonyl-benzene (MN2) was prepared in overall yields of >70%, using a two-step procedure similar to the procedure used for synthesizing MyoNovin.

2-(3,4-Bis-nitrooxy-butoxy)-benzoic acid (MN3) and

2-{3-[3,-bis(nitrooxy)butoxy]phenyl}-acetamide (MN4) have been synthesized using a three-step and four- step procedure, respectively, both in overall yields >70%.

(2) In the present study, an in vitro muscle-fiber culture study was established with the number of BrdU+ SCs through treated muscle fibers with various treatment including ISDN, DMSO, MyoNovin and its analogs. This in vitro muscle fiber culture study demonstrated that two of these MyoNovin analogs – MN2 and MN3 have higher bioactivity than MyoNovin, while MN4 showed slightly decrease when compare with MyoNovin. This observation has presented evidence implicating the structure modification influence bioactivity in different degree.

(3) To test the hypothesis that structural modification may give rise to enhanced water solubility,

water solubility studies were conducted. The result that increased water solubility of all three MyoNovin analogs suggests that these structural modifications indeed enhance the water solubility of MyoNovin.

Bibliography

1. Report on Seniors' falls in Canada: Public Health Agency of Canada; 2005.
2. Canada Year Book: Statistics Canada; 2012.
3. Canadian Community Health Survey – Annual Component: Statistics Canada; 2009-2010.
4. Falls Prevention in Older Age. 2014; http://www.who.int/ageing/projects/falls_prevention_older_age/en/.
5. Rosenberg IH. Sarcopenia: Origins and Clinical Relevance. *Clinics in Geriatric Medicine.* 8// 2011;27(3):337-339.
6. Falls & Related Injuries among Older Canadians: Fall-related Hospitalizations & Prevention Initiatives: Public Health Agency of Canada; 2010.
7. Roth SM, Ferrell RF, Hurley BF. Strength training for the prevention and treatment of sarcopenia. *The journal of nutrition, health & aging.* 2000;4(3):143-155.
8. Evans WJ. Skeletal muscle loss: cachexia, sarcopenia, and inactivity. *The American journal of clinical nutrition.* Apr 2010;91(4):1123s-1127s.
9. Landi F, Cruz-Jentoft AJ, Liperoti R, et al. Sarcopenia and mortality risk in frail older persons aged 80 years and older: results from ilSIRENTE study. *Age and ageing.* Mar 2013;42(2):203-209.
10. Acharyya S, Ladner KJ, Nelsen LL, et al. Cancer cachexia is regulated by selective targeting of skeletal muscle gene products. *The Journal of clinical investigation.* Aug 2004;114(3):370-378.
11. Du J, Wang X, Miereles C, et al. Activation of caspase-3 is an initial step triggering accelerated muscle proteolysis in catabolic conditions. *The Journal of clinical investigation.* Jan 2004;113(1):115-123.
12. Pickering WP, Price SR, Bircher G, Marinovic AC, Mitch WE, Walls J. Nutrition in CAPD: serum bicarbonate and the ubiquitin-proteasome system in muscle. *Kidney international.* Apr 2002;61(4):1286-1292.
13. Morley JE, Kaiser FE, Perry HM, 3rd, et al. Longitudinal changes in testosterone, luteinizing hormone, and follicle-stimulating hormone in healthy older men. *Metabolism: clinical and experimental.* Apr 1997;46(4):410-413.
14. Giovannucci E, Pollak M, Liu Y, et al. Nutritional predictors of insulin-like growth factor I and their relationships to cancer in men. *Cancer epidemiology, biomarkers & prevention : a publication of the American Association for Cancer Research,*

cosponsored by the American Society of Preventive Oncology. Feb 2003;12(2):84-89.
15. Zimmers TA, Davies MV, Koniaris LG, et al. Induction of cachexia in mice by systemically administered myostatin. *Science (New York, N.Y.).* May 24 2002;296(5572):1486-1488.
16. Mitch WE, Goldberg AL. Mechanisms of muscle wasting. The role of the ubiquitin-proteasome pathway. *The New England journal of medicine.* Dec 19 1996;335(25):1897-1905.
17. Iannuzzi-Sucich M, Prestwood KM, Kenny AM. Prevalence of sarcopenia and predictors of skeletal muscle mass in healthy, older men and women. *The journals of gerontology. Series A, Biological sciences and medical sciences.* Dec 2002;57(12):M772-777.
18. Lang T, Streeper T, Cawthon P, Baldwin K, Taaffe DR, Harris TB. Sarcopenia: etiology, clinical consequences, intervention, and assessment. *Osteoporosis international : a journal established as result of cooperation between the European Foundation for Osteoporosis and the National Osteoporosis Foundation of the USA.* Apr 2010;21(4):543-559.
19. Lainscak M, Podbregar M, Anker SD. How does cachexia influence survival in cancer, heart failure and other chronic diseases? *Current opinion in supportive and palliative care.* Dec 2007;1(4):299-305.
20. Waldeyer W. Ueber die Veränderungen der quergestreiften Muskeln bei der Entzündung und dem Typhusprozess, sowie über die Regeneration derselben nach Substanzdefecten. *Archiv f. pathol. Anat.* 1865/12/01 1865;34(4):473-514.
21. Mauro A. Satellite cell of skeletal muscle fibers. *The Journal of biophysical and biochemical cytology.* Feb 1961;9:493-495.
22. Carlson BM, Faulkner JA. The regeneration of skeletal muscle fibers following injury: a review. *Medicine and science in sports and exercise.* 1983;15(3):187-198.
23. Tajbakhsh S. Skeletal muscle stem cells in developmental versus regenerative myogenesis. *Journal of internal medicine.* Oct 2009;266(4):372-389.
24. Janssen I, Heymsfield SB, Wang ZM, Ross R. Skeletal muscle mass and distribution in 468 men and women aged 18-88 yr. *Journal of applied physiology (Bethesda, Md. : 1985).* Jul 2000;89(1):81-88.
25. Brand-Saberi B. *Vertebrate myogenesis*. Springer: Berlin ;; 2002.
26. Buckingham M, Bajard L, Chang T, et al. The formation of skeletal muscle: from somite to limb. *Journal of anatomy.* Jan 2003;202(1):59-68.
27. Voss L, DaSilva M, Trafton PG. Bilateral femoral neck stress fractures in an amenorrheic athlete. *American journal of orthopedics (Belle Mead, N.J.).* Nov

1997;26(11):789-792.
28. Mourkioti F, Rosenthal N. IGF-1, inflammation and stem cells: interactions during muscle regeneration. *Trends in immunology.* Oct 2005;26(10):535-542.
29. Charge SB, Rudnicki MA. Cellular and molecular regulation of muscle regeneration. *Physiol Rev.* Jan 2004;84(1):209-238.
30. Armstrong RB. Initial events in exercise-induced muscular injury. *Medicine and science in sports and exercise.* Aug 1990;22(4):429-435.
31. Bruton JD, Lannergren J, Westerblad H. Mechanisms underlying the slow recovery of force after fatigue: importance of intracellular calcium. *Acta physiologica Scandinavica.* Mar 1998;162(3):285-293.
32. McClung JM, Davis JM, Carson JA. Ovarian hormone status and skeletal muscle inflammation during recovery from disuse in rats. *Experimental physiology.* Jan 2007;92(1):219-232.
33. Kurek JB, Bower JJ, Romanella M, Koentgen F, Murphy M, Austin L. The role of leukemia inhibitory factor in skeletal muscle regeneration. *Muscle & nerve.* Jul 1997;20(7):815-822.
34. Floss T, Arnold HH, Braun T. A role for FGF-6 in skeletal muscle regeneration. *Genes & development.* Aug 15 1997;11(16):2040-2051.
35. Milner DJ, Cameron JA. Muscle repair and regeneration: stem cells, scaffolds, and the contributions of skeletal muscle to amphibian limb regeneration. *Current topics in microbiology and immunology.* 2013;367:133-159.
36. Volonte D, Liu Y, Galbiati F. The modulation of caveolin-1 expression controls satellite cell activation during muscle repair. *FASEB journal : official publication of the Federation of American Societies for Experimental Biology.* Feb 2005;19(2):237-239.
37. Anderson JE. A role for nitric oxide in muscle repair: nitric oxide-mediated activation of muscle satellite cells. *Molecular biology of the cell.* May 2000;11(5):1859-1874.
38. Allbrook DB, Han MF, Hellmuth AE. Population of muscle satellite cells in relation to age and mitotic activity. *Pathology.* Jul 1971;3(3):223-243.
39. Kelly AM. Perisynaptic satellite cells in the developing and mature rat soleus muscle. *The Anatomical record.* Apr 1978;190(4):891-903.
40. Cornelison DD, Wold BJ. Single-cell analysis of regulatory gene expression in quiescent and activated mouse skeletal muscle satellite cells. *Developmental biology.* Nov 15 1997;191(2):270-283.
41. Bischoff R. Proliferation of muscle satellite cells on intact myofibers in culture.

Developmental biology. May 1986;115(1):129-139.
42. Umemura Y, Ishiko T, Yamauchi T, Kurono M, Mashiko S. Five jumps per day increase bone mass and breaking force in rats. *Journal of bone and mineral research : the official journal of the American Society for Bone and Mineral Research.* Sep 1997;12(9):1480-1485.
43. Fyfe I, Stanish WD. The use of eccentric training and stretching in the treatment and prevention of tendon injuries. *Clinics in sports medicine.* Jul 1992;11(3):601-624.
44. Nagata Y, Partridge TA, Matsuda R, Zammit PS. Entry of muscle satellite cells into the cell cycle requires sphingolipid signaling. *J Cell Biol.* Jul 17 2006;174(2):245-253.
45. Loh KC, Leong WI, Carlson ME, et al. Sphingosine-1-phosphate enhances satellite cell activation in dystrophic muscles through a S1PR2/STAT3 signaling pathway. *PloS one.* 2012;7(5):e37218.
46. Wozniak AC, Anderson JE. Nitric oxide-dependence of satellite stem cell activation and quiescence on normal skeletal muscle fibers. *Developmental dynamics : an official publication of the American Association of Anatomists.* Jan 2007;236(1):240-250.
47. Pisconti A, Brunelli S, Di Padova M, et al. Follistatin induction by nitric oxide through cyclic GMP: a tightly regulated signaling pathway that controls myoblast fusion. *J Cell Biol.* Jan 16 2006;172(2):233-244.
48. Perdiguero E, Ruiz-Bonilla V, Gresh L, et al. Genetic analysis of p38 MAP kinases in myogenesis: fundamental role of p38alpha in abrogating myoblast proliferation. *The EMBO journal.* Mar 7 2007;26(5):1245-1256.
49. Daffner RH, Pavlov H. Stress fractures: current concepts. *American Journal of Roentgenology.* 1992/08/01 1992;159(2):245-252.
50. Schmalbruch H. THE SATELLITE CELL OF SKELETAL MUSCLE FIBRES. *Braz. J. morphol. Sci.* 2006;23(2):159-172.
51. Bennett JH, Morgan MJ, Whawell SA, et al. Metalloproteinase expression in normal and malignant oral keratinocytes: stimulation of MMP-2 and -9 by scatter factor. *European journal of oral sciences.* Aug 2000;108(4):281-291.
52. Camp RL, Rimm EB, Rimm DL. Met expression is associated with poor outcome in patients with axillary lymph node negative breast carcinoma. *Cancer.* Dec 1 1999;86(11):2259-2265.
53. Bowers DC, Fan S, Walter KA, et al. Scatter factor/hepatocyte growth factor protects against cytotoxic death in human glioblastoma via phosphatidylinositol 3-kinase- and AKT-dependent pathways. *Cancer research.* Aug 1 2000;60(15):4277-4283.
54. Kujawa M, Baran W, Jankowska-Steifer E. Morphometric ultrastructural analysis of

satellite cells in denervated rat soleus muscle. *Experimental and molecular pathology.* Apr 2004;76(2):166-172.

55. Ambiel CR, Alves-Do-Prado W. Neuromuscular facilitation and blockade induced by L-arginine and nitric oxide in the rat isolated diaphragm. *General pharmacology.* May 1997;28(5):789-794.
56. Boczkowski J, Lanone S, Ungureanu-Longrois D, Danialou G, Fournier T, Aubier M. Induction of diaphragmatic nitric oxide synthase after endotoxin administration in rats: role on diaphragmatic contractile dysfunction. *The Journal of clinical investigation.* Oct 1 1996;98(7):1550-1559.
57. Filippin LI, Cuevas MJ, Lima E, Marroni NP, Gonzalez-Gallego J, Xavier RM. Nitric oxide regulates the repair of injured skeletal muscle. *Nitric oxide : biology and chemistry / official journal of the Nitric Oxide Society.* Jan 1 2011;24(1):43-49.
58. Filippin LI, Cuevas MJ, Lima E, Marroni NP, Gonzalez-Gallego J, Xavier RM. The role of nitric oxide during healing of trauma to the skeletal muscle. *Inflammation research : official journal of the European Histamine Research Society ... [et al.].* Apr 2011;60(4):347-356.
59. Rubinstein I, Abassi Z, Coleman R, Milman F, Winaver J, Better OS. Involvement of nitric oxide system in experimental muscle crush injury. *The Journal of clinical investigation.* Mar 15 1998;101(6):1325-1333.
60. Rigamonti E, Touvier T, Clementi E, Manfredi AA, Brunelli S, Rovere-Querini P. Requirement of inducible nitric oxide synthase for skeletal muscle regeneration after acute damage. *Journal of immunology (Baltimore, Md. : 1950).* Feb 15 2013;190(4):1767-1777.
61. Tidball JG, Wehling-Henricks M. Expression of a NOS transgene in dystrophin-deficient muscle reduces muscle membrane damage without increasing the expression of membrane-associated cytoskeletal proteins. *Molecular genetics and metabolism.* Aug 2004;82(4):312-320.
62. Brenman JE, Chao DS, Xia H, Aldape K, Bredt DS. Nitric oxide synthase complexed with dystrophin and absent from skeletal muscle sarcolemma in Duchenne muscular dystrophy. *Cell.* Sep 8 1995;82(5):743-752.
63. Colussi C, Mozzetta C, Gurtner A, et al. HDAC2 blockade by nitric oxide and histone deacetylase inhibitors reveals a common target in Duchenne muscular dystrophy treatment. *Proceedings of the National Academy of Sciences.* December 9, 2008 2008;105(49):19183-19187.
64. Clementi E. Role of nitric oxide and its intracellular signalling pathways in the control of Ca2+ homeostasis. *Biochemical pharmacology.* Mar 15

1998;55(6):713-718.
65. Johnson RM, Lincoln TM. Effects of nitroprusside, glyceryl trinitrate, and 8-bromo cyclic GMP on phosphorylase a formation and myosin light chain phosphorylation in rat aorta. *Molecular pharmacology.* Mar 1985;27(3):333-342.
66. Nisoli E, Tonello C, Cardile A, et al. Calorie restriction promotes mitochondrial biogenesis by inducing the expression of eNOS. *Science (New York, N.Y.).* Oct 14 2005;310(5746):314-317.
67. Nisoli E, Falcone S, Tonello C, et al. Mitochondrial biogenesis by NO yields functionally active mitochondria in mammals. *Proceedings of the National Academy of Sciences of the United States of America.* Nov 23 2004;101(47):16507-16512.
68. Csete M, Walikonis J, Slawny N, et al. Oxygen-mediated regulation of skeletal muscle satellite cell proliferation and adipogenesis in culture. *Journal of Cellular Physiology.* 2001;189(2):189-196.
69. De Palma C, Clementi E. Nitric oxide in myogenesis and therapeutic muscle repair. *Molecular neurobiology.* Dec 2012;46(3):682-692.
70. Sun Y, Oberley LW. Redox regulation of transcriptional activators. *Free Radical Biology and Medicine.* // 1996;21(3):335-348.
71. Espey MG, Miranda KM, Feelisch M, et al. Mechanisms of cell death governed by the balance between nitrosative and oxidative stress. *Annals of the New York Academy of Sciences.* 2000;899:209-221.
72. Vasilaki A, Jackson MJ. Role of reactive oxygen species in the defective regeneration seen in aging muscle. *Free radical biology & medicine.* Dec 2013;65:317-323.
73. Lee S, Shin HS, Shireman PK, Vasilaki A, Van Remmen H, Csete ME. Glutathione-peroxidase-1 null muscle progenitor cells are globally defective. *Free radical biology & medicine.* Oct 1 2006;41(7):1174-1184.
74. Frandsen U, Lopez-Figueroa M, Hellsten Y. Localization of nitric oxide synthase in human skeletal muscle. *Biochemical and biophysical research communications.* Oct 3 1996;227(1):88-93.
75. Wang GQ, Burczynski FJ, Hasinoff BB, Zhang KD, Lu QL, Anderson JE. Development of a Nitric Oxide-Releasing Analogue of the Muscle Relaxant Guaifenesin for Skeletal Muscle Satellite Cell Myogenesis. *Mol Pharmaceut.* May-Jun 2009;6(3):895-904.
76. Chandrashekar Giliyar DTF, Shanthakumar Tyavanagimatt. Challenges & Opportunities in Oral Delivery of Poorly Water-Soluble Drugs. *Drug Delivery Technology.* 2006;6(1):57-63.
77. Sumida K, Igarashi Y, Toritsuka N, et al. Effects of DMSO on gene expression in human and rat hepatocytes. *Human & experimental toxicology.* Oct

2011;30(10):1701-1709.
78. Heerdt BG, Houston MA, Rediske JJ, Augenlicht LH. Steady-state levels of mitochondrial messenger RNA species characterize a predominant pathway culminating in apoptosis and shedding of HT29 human colonic carcinoma cells. *Cell growth & differentiation : the molecular biology journal of the American Association for Cancer Research.* Jan 1996;7(1):101-106.
79. Edward Kerns LD. *Drug-like Properties: Concepts, Structure Design and Methods from ADME to Toxicity Optimization*: elsevier; 2008.
80. Sareen S, Mathew G, Joseph L. Improvement in solubility of poor water-soluble drugs by solid dispersion. *International journal of pharmaceutical investigation.* Jan 2012;2(1):12-17.
81. V. BALSSKPS. Enhancement of Solubility: A Pharmaceutical Overview. *Der Pharmacia Lettre.* 2010;2(2):310-318.
82. Rytting E, Lentz K, Chen X-Q, Qian F, Venkatesh S. Aqueous and cosolvent solubility data for drug-like organic compounds. *AAPS J.* 2005/03/01 2005;7(1):E78-E105.
83. Delgado DR, MartÍNez R F. THERMODYNAMIC STUDY OF THE SOLUBILITY OF SODIUM SULFADIAZINE IN SOME ETHANOL + WATER COSOLVENT MIXTURES. *Vitae.* 2010;17:191-198.
84. Sweetana S, Akers MJ. Solubility principles and practices for parenteral drug dosage form development. *PDA journal of pharmaceutical science and technology / PDA.* Sep-Oct 1996;50(5):330-342.
85. Gibaldi Milo ML, Archana Desai. *Gibaldi's drug delivery systems in pharmaceutical care.*: American Society of Health-System Pharmacists; 2007.
86. Hajduk PJ, Sauer DR. Statistical analysis of the effects of common chemical substituents on ligand potency. *Journal of medicinal chemistry.* Feb 14 2008;51(3):553-564.
87. Baka E, Comer JEA, Takács-Novák K. Study of equilibrium solubility measurement by saturation shake-flask method using hydrochlorothiazide as model compound. *Journal of Pharmaceutical and Biomedical Analysis.* 1/22/ 2008;46(2):335-341.
88. Lipinski CA, Lombardo F, Dominy BW, Feeney PJ. Experimental and computational approaches to estimate solubility and permeability in drug discovery and development settings. *Advanced Drug Delivery Reviews.* 1/15/ 1997;23(1–3):3-25.
89. Seadeek C, Ando H, Bhattachar SN, Heimbach T, Sonnenberg JL, Blackburn AC. Automated approach to couple solubility with final pH and crystallinity for pharmaceutical discovery compounds. *J Pharm Biomed Anal.* Apr 11 2007;43(5):1660-1666.

90. Taub ME, Kristensen L, Frokjaer S. Optimized conditions for MDCK permeability and turbidimetric solubility studies using compounds representative of BCS classes I–IV. *European Journal of Pharmaceutical Sciences.* 5// 2002;15(4):331-340.
91. Bergstrom CA, Luthman K, Artursson P. Accuracy of calculated pH-dependent aqueous drug solubility. *European journal of pharmaceutical sciences : official journal of the European Federation for Pharmaceutical Sciences.* Aug 2004;22(5):387-398.
92. Dehring KA, Workman HL, Miller KD, Mandagere A, Poole SK. Automated robotic liquid handling/laser-based nephelometry system for high throughput measurement of kinetic aqueous solubility. *J Pharm Biomed Anal.* Nov 15 2004;36(3):447-456.
93. Pitt A. High-throughput screening to determine aqueous drug solubility: the author describes an aqueous solubility screening assay methodology that uses 96-well plates and compares performance to the conventional shake-flask method. *Pharmaceutical Discovery.* Jan 2005;5:46+.
94. Fligge TA, Schuler A. Integration of a rapid automated solubility classification into early validation of hits obtained by high throughput screening. *J Pharm Biomed Anal.* Oct 11 2006;42(4):449-454.
95. Avdeef A, Berger CM. pH-metric solubility. 3. Dissolution titration template method for solubility determination. *European journal of pharmaceutical sciences : official journal of the European Federation for Pharmaceutical Sciences.* Dec 2001;14(4):281-291.
96. Avdeef A, Berger C, Brownell C. pH-Metric Solubility. 2: Correlation Between the Acid-Base Titration and the Saturation Shake-Flask Solubility-pH Methods. *Pharmaceutical research.* 2000/01/01 2000;17(1):85-89.
97. Box KJ, Völgyi G, Baka E, Stuart M, Takács-Novák K, Comer JEA. Equilibrium versus kinetic measurements of aqueous solubility, and the ability of compounds to supersaturate in solution—a validation study. *Journal of pharmaceutical sciences.* 2006;95(6):1298-1307.
98. Avdeef A, Berger CM, Brownell C. pH-metric solubility. 2: correlation between the acid-base titration and the saturation shake-flask solubility-pH methods. *Pharmaceutical research.* Jan 2000;17(1):85-89.
99. Stuart M, Box K. Chasing equilibrium: measuring the intrinsic solubility of weak acids and bases. *Analytical chemistry.* Feb 15 2005;77(4):983-990.
100. Kerns EH, Di L. Pharmaceutical profiling in drug discovery. *Drug discovery today.* Apr 1 2003;8(7):316-323.

101. Sugano K, Kato T, Suzuki K, Keiko K, Sujaku T, Mano T. High throughput solubility measurement with automated polarized light microscopy analysis. *Journal of pharmaceutical sciences.* Oct 2006;95(10):2115-2122.
102. Feelisch M, Kelm M. Biotransformation of organic nitrates to nitric oxide by vascular smooth muscle and endothelial cells. *Biochemical and biophysical research communications.* Oct 15 1991;180(1):286-293.
103. Kurz MA, Boyer TD, Whalen R, Peterson TE, Harrison DG. Nitroglycerin metabolism in vascular tissue: role of glutathione S-transferases and relationship between NO. and NO2- formation. *Biochemical Journal.* 1993;292(Pt 2):545-550.
104. Avdeef A, Bendels S, Tsinman O, Tsinman K, Kansy M. Solubility-excipient classification gradient maps. *Pharmaceutical research.* Mar 2007;24(3):530-545.
105. Glomme A, Marz J, Dressman JB. Comparison of a miniaturized shake-flask solubility method with automated potentiometric acid/base titrations and calculated solubilities. *Journal of pharmaceutical sciences.* Jan 2005;94(1):1-16.
106. Thomas GD, Ye J, De Nardi C, Monopoli A, Ongini E, Victor RG. Treatment with a nitric oxide-donating NSAID alleviates functional muscle ischemia in the mouse model of Duchenne muscular dystrophy. *PloS one.* 2012;7(11):e49350.
107. Sciorati C, Miglietta D, Buono R, et al. A dual acting compound releasing nitric oxide (NO) and ibuprofen, NCX 320, shows significant therapeutic effects in a mouse model of muscular dystrophy. *Pharmacological research : the official journal of the Italian Pharmacological Society.* Sep 2011;64(3):210-217.

Appendix 1

Collagenase medium: 0.2% collagenase, 1X Dulbecco's Modified Eagle's Medium (DMEM), 10% fetal bovine serum (FBS), 2% chick embryo extract (CEE), 1% antibiotic/antimycotic and 0.1% gentamycin.

Proliferation medium: L-15 medium, 10% FBS, 2% CEE, 1% antibiotic/antimycotic and 0.1% gentamycin.

Basal growth medium: L-15 medium, 20% controlled replacement serum-2 (50X) (Sigma Aldrich, St. Louis, MO), 1% FBS, 1% antibiotic/antimycotic and 0.1% gentamycin.

0.1M Phosphate buffered saline: 80 g NaCl, 2 g KCl, 26.8 g $Na_2HPO_4.7H_2O$, 2.4 g KH_2PO_4 in 800 ml of dd H_2O and adjust pH to 7.4. Add volume to 1L with dd H_2O.

5% acid alcohol: 90% absolute ethanol, 5% glacial acetic acid, 5% dd H_2O.

0.1M Tris buffered saline: 61g tris base and 90g NaCl in 800 ml ddH_2O and pH is adjusted to 8.4

using concentrated HCl. Add volume to 1L with dd H_2O.

Primary antibody buffer solution: 1%BSA, 0.1% cold fish skin gelatin, 0.5% Triton X- 100, 0.05% sodium azide.

Secondary antibody buffer solution: 0.01M PBS, 0.05% Tween 20, pH7